

Received September 19, 2020, accepted October 5, 2020, date of publication October 9, 2020, date of current version October 21, 2020.

Digital Object Identifier 10.1109/ACCESS.2020.3029943

Machine Learning Based Energy Management Model for Smart Grid and Renewable Energy Districts

WAQAR AHMED¹, (Associate Member, IEEE), HAMMAD ANSARI², BILAL KHAN¹, ZAHID ULLAH³, SAHIBZADA MUHAMMAD ALI¹, CHAUDHRY ARSHAD ARSHAD MEHMOOD¹, MUHAMMAD B. QURESHI¹, (Member, IEEE), IQRAR HUSSAIN³, MUHAMMAD JAWAD⁴, MUHAMMAD USMAN SHAHID KHAN⁵, (Member, IEEE), AMJAD ULLAH⁶, AND RAHEEL NAWAZ⁷

¹Department of Electrical Engineering, CUI Abbottabad Campus, Abbottabad 22060, Pakistan

²Department of Mathematics and Natural Sciences, Centre for Applied Mathematics and Bioinformatics, Gulf University for Science and Technology, Mubarak Al-Abdullah 32093, Kuwait

³Department of Electrical Engineering, UMT Lahore Sialkot Campus, Lahore 54770, Pakistan

⁴Department of Electrical Engineering, CUI Lahore Campus, Lahore 54000, Pakistan

⁵Department of Computer Science, CUI Abbottabad Campus, Khyber Pakhtunkhwa 22060, Pakistan

⁶Department of Electrical Engineering, UET Peshawar, Peshawar 25120, Pakistan

⁷Manchester Metropolitan University, Manchester M15 6BH, U.K.

Corresponding author: Muhammad B. Qureshi (bilalqureshi@cuiatd.edu.pk)

ABSTRACT The combination of renewable energy sources and prosumer-based smart grid is a sustainable solution to cater to the problem of energy demand management. A pressing need is to develop an efficient Energy Management Model (EMM) that integrates renewable energy sources with smart grids. However, the variable scenarios and constraints make this a complex problem. Machine Learning (ML) methods can often model complex and non-linear data better than the statistical models. Therefore, developing an ML algorithm for the EMM is a suitable option as it reduces the complexity of the EMM by developing a single trained model to predict the performance parameters of EMM for multiple scenarios. However, understanding latent correlations and developing trust in highly complex ML models for designing EMM within the stochastic prosumer-based smart grid is still a challenging task. Therefore, this paper integrates ML and Gaussian Process Regression (GPR) in the EMM. At the first stage, an optimization model for Prosumer Energy Surplus (PES), Prosumer Energy Cost (PEC), and Grid Revenue (GR) is formulated to calculate base performance parameters (PES, PEC, and GR) for the training of the ML-based GPR model. In the second stage, stochasticity of renewable energy sources, load, and energy price, same as provided by the Genetic Algorithm (GA) based optimization model for PES, PEC, and GR, and base performance parameters act as input covariates to produce a GPR model that predicts PES, PEC, and GR. Seasonal variations of PES, PEC, and GR are incorporated to remove hitches from seasonal dynamics of prosumers energy generation and prosumers energy consumption. The proposed adaptive Service Level Agreement (SLA) between energy prosumers and the grid benefits both these entities. The results of the proposed model are rigorously compared with conventional optimization (GA and PSO) based EMM to prove the validity of the proposed model.

INDEX TERMS Prosumer, smart grid, machine learning, energy districts, service level agreement, smart contract, optimization, Gaussian process regression, energy management model.

The associate editor coordinating the review of this manuscript and approving it for publication was Tallha Akram¹.

I. INTRODUCTION

According to the US Department of Energy (DoE), the existing electric system is congested, insufficient, and unable to

satisfy future energy demands. The reliability of the grid has become the most important factor, as the conventional grid has been transforming into a smarter grid over several years. Therefore, we need online operations for smart grid operations to become more online and keep the previous records of environmental parameters, electricity generation, and energy demand to predict future energy needs.

Stochastically varying energy demand tends to cause a mismatch between energy demand and energy supply while resulting in unstable grid operation. Incentivization is one of the energy management techniques in which prosumers (small scale energy generating and utilizing consumers also known as Energy Districts (EDs)) are incentivized to schedule their load in specified time intervals (demand-side management). However, the integration of renewable energy resources with existing grids can cause irregularity and intermittency because of various factors, such as variable wind speed in the case of wind power generation and variable solar irradiance in the case of solar power generation.

Over the last few decades, researchers have been investigating how to design a comprehensive Energy Management Model (EMM) that benefits both grid and prosumers. Over time, energy management techniques and optimization algorithms are incorporated in the EMMs to deliver reliable, clean, and affordable energy [1], [2]. The use of optimization algorithms in power systems is to balance energy demand and supply to satisfy economic load dispatch, system stability, and Quality-of-Service (QoS) [2]. A good optimization technique needs completely known criteria, system requirements, and specifications. If the system specification changes, such as variable energy supply due to renewable energy sources and variable prosumer requirements, then the optimization problem needs a reformulation to fit new variations. Therefore, an optimized algorithm is not fit for all parameter variations and hard to deploy and test in real-time.

Significant research has been conducted in the area of energy management between prosumers and smart grid utilities [1]–[4]. Still, crucial improvements are needed in the EMMs, energy efficient algorithms, communication, energy estimation, and control. Congestion and reliability are the key concerns in the EMM presented in [3], [4]. An EMM with multiple layers, monitoring, communication, and smart metering was analyzed irrespective of the stochasticity of renewable energy sources [5]. A framework to enhance prosumer participation was deployed in [6] and [7] but the market for transactive environments poses challenges, such as finagling energy clearing prices and exchange of capital between prosumers; therefore, some decision restrictions are imposed on a prosumer operation that can degrade integrity. Trustworthy and quality aspects were of great importance for smooth and appropriate stakeholder's role as maintained in [8] by presenting Service Level Agreement (SLA); however, dynamic Region of Convergence (ROC) and Region of Divergence (ROD) were not analyzed.

Usually, the energy transactions are practiced within prosumers, clusters of prosumers, prosumers and utilities,

clusters, and utilities. In [9], the authors implemented a demand response program for energy management to achieve maximum utilization of renewable energy sources. Similarly, in [10], the demand response programs are used to decrease the lumped cost of prosumer-based microgrids. Price based demand response programs included real-time pricing and day-ahead pricing schemes were also incentivized for prosumers. In this perspective, an energy storage system coordinated for real-time and day-ahead scheduling of industrial complex was examined for bidirectional energy flow [11]. The Machine Learning (ML) models were developed to practically analyze the test-bed results for demand response algorithms [12].

Balancing energy demand with energy supply is another important parameter to maximize the mutual benefits of stakeholders. As minimizing energy exchange is more beneficial than reducing energy cost, an objective function for maximizing the balance between energy demand and energy supply was developed in [13]. To create awareness about the demand-supply situation in the distribution system, the authors have introduced phasor measurement units. The authors in [14] presented a solution to the problem of arranging a large dataset from phasor measurement units into information and then matching the information with a practical case. In [15], the risk of failure for power systems and respective components was also analyzed by developing a generalized ML model from historical data of the New York power grid.

The ML algorithms are widely used in the smart grid environment for numerous problems, such as prediction, energy management, and reliability. For example, work in [16] predicted the day-ahead energy consumption of air conditioners within the smart grid to analyze the effectiveness of the ML. Furthermore, the efficiency of the hybrid Support Vector Machine (SVM) and Artificial Neural Network (ANN) was explored for the protective setting and network topology to ensure the reliability of the microgrids [17]. Assaults of data integrity on communication networks were predicted [18]–[23]; this work evaluated unsupervised ML using an isolation forest algorithm.

Although the above works are successful in modeling and analyzing the EMMs for prosumers and smart grids, they still have not developed a comprehensive, ML-based EMM that also incorporates important features of EMM, such as Smart Contracts (SCs) to stream-line demand-supply management and a well-defined Service Level Agreements (SLAs) between smart grid and prosumers. The SLAs must contain multiple ROCs and RODs with seasonal variations for smooth bidirectional energy flow between smart grid and prosumers having renewable energy sources.

As illustrated above, optimization algorithms require reformulation to handle the parameter variations associated with smart grids and prosumers, and seasonal variations in real-time, which are often not modelled in optimization formulation. The ML is one of the solutions to cope with the problem of parameter variations, such as renewable power generation,

demand change, and environmental and seasonal drifts. Therefore, developing an ML algorithm for the EMM is a suitable option as it reduces the complexity of the EMM by developing a single trained model to predict the performance parameters of EMM for multiple scenarios. Moreover, the integration of the ML algorithm with optimization techniques can learn multiple formulations and criteria both online and offline. However, understanding latent correlations and developing trust in highly complex ML models for designing EMM within the stochastic prosumer-based smart grid is still a challenging task. Therefore, integration of ML and Gaussian Process Regression (GPR) in the EMM along with an optimization technique is the comprehensive solution of the above-mentioned problem. In light of the above-stated summary, the main contributions of the paper are:

- Due to the ability of the ML algorithms to learn multiple formulations and measures from data, such as intermittent of renewable power generation, plug and play facilities, prosumer activities, and complex power system formulations both in online and offline modes, an EMM is developed for mutual energy trade between smart grid and EDs. The output parameters considered for the EMM are prosumer energy surplus (PES), prosumer energy cost (PEC), and grid revenue GR to increase the mutual benefits of smart grids and EDs. The optimization algorithms tested for the above-stated purpose are the Genetic Algorithm (GA) and Particle Swarm Optimization (PSO).
- To develop a trustful understanding of latent correlations between response parameters and input covariates, a Gaussian Process Regression (GPR) is integrated with the ML algorithm.
- An ML-based stochastic adaptive-service level agreement (SA-SLA) is designed that incorporates stochasticity of renewable energy sources by developing multiple SCs based smart SLAs with own convergence and divergence regions for three different EDs studied. The proposed ML-GPR integrated with optimization algorithm based EMM is tested and compared against the conventional optimization based EMM in terms of measuring parameters, such as PES, PEC, and GR. The proposed model outperformed the conventional model due to reduced energy consumption cost, reduced surplus energy, and maximization of grid revenue.
- Statistical analysis using box plots, Q-Q plots, and tabular analysis are performed to prove the validity of the ML-GPR integrated with optimization algorithm in developing a comprehensive EMM. Moreover, seasonal variations of the PES, PEC, and GR are incorporated to remove hitches from the environmental dynamics of different seasons.

The paper is organized as follows: Section 2 discusses EMM within smart grid incorporating system model, SCs, SA-SLA, and environmental shifts; Section 3 formulates the optimization model, wind energy estimation, solar energy estimation, PES, PEC, and GR of the smart grid; Section 4 elaborates

GPR based EMM designed to estimate response parameters (PES, PEC, GR); Section 5 details performance validation including data analysis, seasonal variations of PES, PEC, and GR, statistical analysis, and tabular analysis, and finally, Section 6 concludes the paper.

II. ENERGY MANAGEMENT MODEL FOR SMART GRID AND ENERGY DISTRICTS

Energy management means monitoring, communicating, controlling, and optimizing the performance of electrical energy. The development of EMM positively enhances the performance of electric generation, transmission, distribution, and utilization. A generalized smart grid model with domains and sub-domains with the proposed EMM incorporating SLA within the smart grid is presented in this section.

A. SYSTEM MODEL

An electrical grid comprising of renewable energy sources, smart appliances, smart meters, and energy efficient resources is called the smart grid [24]–[26]. Smart grid domains include bulk and non-bulk generation, customers, service provider, distribution, transmission, foundation support system, markets, and operations. Advance protection, communication system, customer enabling, energy storage system, micro, and nano grids, plug-in vehicles, distributed energy sources, and demand response programs are sub-domains of the smart grid [27]. In the smart grid, fossil fuel based and renewable based energy sources (prosumers) are utilized to produce small scale and large-scale energy, and there is a bidirectional energy flow between stakeholders [28].

Three EDs, with the facility of renewable energy sources, are considered in this paper. ED1 and ED2 are located at Copano Bay, Texas, US while ED3 is located at Brownsville, Texas, US. Wind Turbines (WTs) generate energy for ED1 and ED2 while solar PV arrays produce energy for ED3 in the smart grid model. Bidirectional energy and information flow between EDs and utility through Coalition Manager (CM) under the SLA. Prosumers pay for net energy consumption each month. Optimization based EMM and ML-based EMM for smart grid and renewable Eds are proposed in this paper to show the effectiveness of the ML approach in the smart grid. The conceptual EMM for bidirectional energy flow between the smart grid and EDs is depicted in Figure 1.

B. SMART CONTRACTS (SCS)

EDs prosumers generate energy and sell their energy surplus to the smart grid (utility) under a contract. Prosumers' energy generation is based on stochastic environmental parameters (wind speed and solar irradiance). Stochastic renewable energy sources of EDs tend to generate time-varying PES. Single contract associates large fluctuations of PES and so is less beneficial to prosumers and smart grid. In respect to stochastic environmental parameters, multiple SCs based on different ranges of PES are developed in this paper.

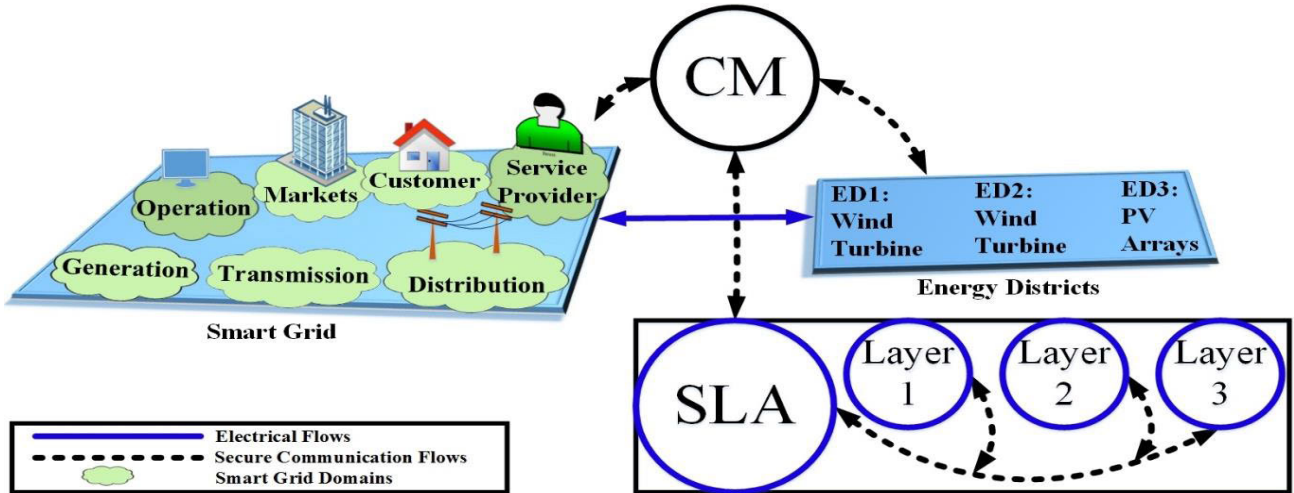


FIGURE 1. Proposed energy management model for EDs and smart grid. ED: Energy District, CM: Coalition Manager, SLA: Service Level Agreement.

Multiple SCs are liable to develop multiple SLAs with their convergence and divergence area and associate fewer fluctuations of PES. Fewer fluctuations of PES ensure stable prosumers operation and make SCs more beneficial to stakeholders. Multiple SCs, based on different ranges of PES are defined as:

$$SCs = \begin{cases} SC_1 & \text{for } 10\% \leq E_S \leq 30\%, \\ SC_2 & \text{for } 31\% \leq E_S \leq 60\%, \\ SC_3 & \text{for } 61\% \leq E_S \leq 100\%. \end{cases} \quad (1)$$

where SC_1 , SC_2 , and SC_3 are smart contract 1, smart contract 2, and smart contract 3 respectively while E_S is Prosumer Energy Surplus (PES). For each mutually agreed SCs, such as SC_1 , SC_2 , and SC_3 , a separate range of energy price (based on prosumer energy cost and prosumer energy surplus) is considered. The high energy contract i.e. SC_3 associates less prosumer energy cost and similarly SC_1 and SC_2 are less energy contract in comparison with SC_3 .

C. STOCHASTIC ADAPTIVE-SERVICE LEVEL AGREEMENT (SA-SLA) DESIGN

A formal contract between service users and service providers is known as Service Level Agreement (SLA). SLA retains the quality and reliability of service by developing trustworthiness between stakeholders. The generalized scenario of SLA is based on some type of contract between stakeholders. In the context of EMM within the smart grid, the EDs and smart grid play the role of stakeholders, and contracts are agreed between them in terms of prosumer energy surplus (PES). SLA for bidirectional transactive energy system between stakeholders is developed based on contracted PES and resulting PEC. As explained earlier, the development of SCs is based on multiple ranges of PES; an SA-SLA comprising of multiple SCs based SLAs is proposed in this paper. Each SC develops a single SLA with unique ROC and ROD. SC with the small contracted value of PES is liable to develop

SLA with high PEC while SC with the large contracted value of PES is liable to develop SLA with less PEC. Moreover, SLA is comprised of three internal layers in communication with CM to play its role of possessing stakeholders under the SLA umbrella.

Layer one is confined to agent descriptions, multiple SCs, constraints regarding stakeholders, rules, and service standards. Following various rules and SCs, stakeholders' facts are converted into a familiar form for layer two meanwhile sending it to layer two for additional accounts. Directions of CM are directly provided to layer two. In time evaluation of layer two is achieved by inspecting information using If-then commands and sending the decision to layer three. Service security, energy management issues, response time, and stakeholder's performance are the most concerning parameters of layer three. CM takes the final decision based on the conclusion drawn from layer three and circulates decisions to stakeholders.

Coalition Manager (CM): Performance of stakeholders is monitored by a central entity of SA-SLA called CM. A strong communication system exists between CM and stakeholders for resourceful energy management. CM perceives the commitment of stakeholders and communicates to keep stakeholders under SLA after critically analyzing SLA layers. CM legalizes the activities of stakeholders by stipulating special rewards and penalties. Penalties and rewards are based on the criterion of Amazon EC2. Violating stakeholders will pay 10% of contracted amount for a 1% delay of total time execution. The penalty will increase from 10% to 30% of the contracted amount for Execution Time Delay (ETD) greater than 1%.

1) MACHINE LEARNING (ML) BASED SA-SLA DESIGN

ML-based SA-SLA is designed using the outcomes of the ML model. GPR based ML model is selected to design the proposed EMM. Complete detail about training and

testing of the GPR model is explained in Section 4 but the summary is provided here for an understanding of how the GPR model achieves the aim of designing SA-SLA. At first, an optimization model is used to calculate input covariates (response variable, prosumers available energy, prosumers load, and pricing) for the training of the GPR model. Repetitive measures of input covariates are computed for complete training and design parameters of GPR are attained using the optimization method. The efficiency of a trained ML model is evaluated in terms of PES, PEC, and GR of the smart grid. Multiple SCs are developed for various ranges of PES. Based on multiple SCs, smart SLAs with different convergence regions are modelled and designed. The role of GPR based SA-SLA merging different layers and multiple smart SLAs is depicted in Figure 1.

D. ENVIRONMENTAL SHIFTS

Disturbances created by humans, animals, and natural ecological progressions disturb the natural environment and creates global issues. Dry bulb temperature, Wind Speed (WS), Solar Irradiance (SI), dew point, and cloud covers are the most basic environmental parameters. In the context of designing an EMM for the smart grid and EDs prosumers, the variations of environmental parameters influence in varying the energy production and energy consumption patterns of prosumers. So, an amalgamation of environmental shifts becomes necessary for the accurate designing of the EMM. In this perspective, this paper analyses environmental shifts in terms of different seasons of the year namely, spring, summer, fall, and winter. PEC, PES, and GR of the smart grid are calculated for each season of the year to unhide their seasonal variations in designing EMM.

III. OPTIMIZATION MODEL FOR EMM PARAMETERS

The energy production of EDs is based on stochastic WS and SI. EDs self-energy demand is a stochastic function of prosumers energy consumption preferences. WS, SI, and prosumer energy demand are considered as base parameters that can vary the response parameters (PES, PEC, and GR). Increasing PES while decreasing PEC and increasing GR is the main objective of the proposed EMM. Although the stochasticity of base parameters creates complexities to achieve the aforementioned objectives, optimization performs well in the scenario of stochasticity [29]. Multi-objective optimization using Genetic Algorithms (GA) is used to optimize PES, PEC, and GR.

Optimization problem 1 (OP1) is about PES, Optimization Problem 2 (OP2) is about PEC, and Optimization Problem 3 (OP3) is about GR. At first, OP1 is solved to optimize PES using prosumer energy management as presented in (9-13). Afterward, based on pre-managed prosumer load, the objective functions of OP2 (PEC) and OP3 (GR) are optimized in (14-18) and (19-22) respectively. The pre-managed prosumer load is used as a convergence criterion that creates a trade-off between PEC, PES, and GR. Therefore, to attain the said objectives, optimization models for PEC,

PES, and GR are formulated in this subsection III.D, III.E, and III. F. Subsection III.A, III.B, and III.C mathematically model Gaussian Energy distribution functions of prosumers, Wind Energy Estimation Model, and Solar Energy Estimation model respectively.

A. GAUSSIAN ENERGY DISTRIBUTION FUNCTIONS OF PROSUMERS

Environmental parameters (WS and SI) exhibit a stochastic pattern. In response to the stochastic behaviour of environmental parameters (WS and SI), SA-SLA incorporates a stochastic function for prosumers energy generation. Prosumers generated energy is captured by using gaussian distribution function because renewable energy approximately follows Gaussian distribution [30] defined as:

$$f_E(e) = ae^{-\frac{(e-\mu_E)^2}{2\sigma_E^2}} \quad (2)$$

where, $a = \frac{1}{\sqrt{2\pi\sigma_E^2}}$ represents the height of the curve's peak that represents the maximum generated energy, μ_E represents mean of prosumers generated energy, and σ_E represents the standard deviation of prosumers generated energy.

According to the central limit theorem, the sum of independent but identically distributed (i.i.d) variables follows a Gaussian distribution. Since the prosumers generated energy entirely depends on the independently varying WS and SI, the random vector associated with prosumers generated energy have values written as:

$$E = (E_{t_1}, E_{t_2}, \dots, E_{t_k}) \quad (3)$$

where $E_{t_1}, E_{t_2}, \dots, E_{t_k}$ are Gaussian variables each representing prosumers generated energy in the time interval t_1, t_2, \dots, t_k . As each component exhibits univariate gaussian distribution, the random vector itself exhibits a multivariate gaussian distribution with k dimensions. A linear combination of random vector components is given as:

$$Y = (d_1 E_{t_1} + \dots + d_k E_{t_k}) \quad (4)$$

For any constant vector $d \in \mathbb{R}^k$ and random variable $Y = d^T$, the random vector follows the multivariate gaussian distribution. The generalized expressions for output power and energy from WT and PV arrays are provided in the following subsections.

B. WIND ENERGY ESTIMATION MODEL

In ED1 and ED2 the energy productions are based on the output power of WT. The actual output power of WT is a function of stochastic WS and rated output power [31]. As rated output power remains the same as tabulated on the nameplate of a specific WT, variations of WS tend to cause multiple ranges of actual power output from WT. A mathematical model for the output power of WT as a function of stochastic WS is

expressed as:

$$G_w = \begin{cases} 0 & v \leq v_i, v \geq v_0 \\ \frac{v - v_i}{v_r - v_i} G_{w_r} & v_i \leq v \leq v_r \\ G_{w_r} & v_r \leq v \leq v_0 \end{cases} \quad (5)$$

where, G_w is actual output power from WT, G_{w_r} is rated output power of WT, v represents wind speed, v_i is cut-in wind speed, v_r is rated wind speed, and v_0 is a cut-out wind speed of WT. The output energy from WT is defined as:

$$E_w = t_w * G_w = t_w \begin{cases} 0 & v \leq v_i, v \geq v_0 \\ \frac{v - v_i}{v_r - v_i} G_{w_r} & v_i \leq v \leq v_r \\ G_{w_r} & v_r \leq v \leq v_0 \end{cases} \quad (6)$$

where, E_w is actual output energy from WT and t_w denotes WT operating time. Visual representation of actual output power from WT is depicted in Figure 2.

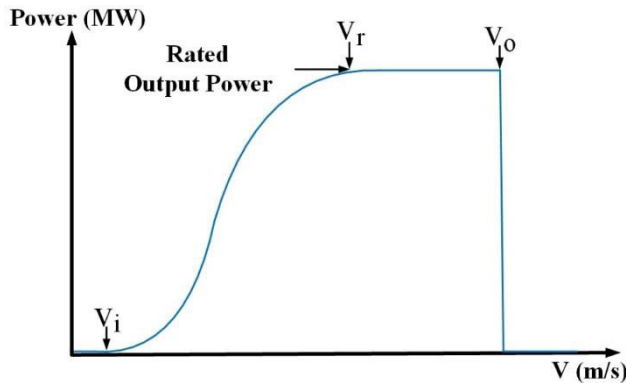


FIGURE 2. Output power curve of wind turbine.

C. SOLAR ENERGY ESTIMATION MODEL

The energy production of ED3 is based on the output power of solar PV arrays. The output power of the PV array is a function of SI, the performance ratio of PV array, the yield of PV array, and a total area of PV array [32]; it is defined as:

$$P_{act} = A * G * PR * r \quad (7)$$

where, P_{act} is actual output power from PV array, A represents the total area of PV array, G represents annual solar irradiance averaged on a tilted axis (in Kw/m^2), r is yield (in %) of the solar array, PR denotes PV array's performance ratio. The output energy from the PV array is defined as:

$$E_{PV} = t_{PV} * P_{act} = t_{PV} * A * G * PR * r. \quad (8)$$

where, E_{PV} is actual output energy from PV array while t_{PV} denotes the operating time of the PV array.

D. PROSUMER ENERGY SURPLUS (PES)

Most prosumers utilize renewable energy sources for energy generation. After meeting the prosumer's energy demand, the extra available energy is known to be PES [34]. Prosumer-based smart grid enables bidirectional energy transactions between prosumer and utility through SLA. Thus, bidirectional energy transactions facilitate prosumers to sell PES at a nominal price [8]. The optimization model for PES is formulated as:

$$\max \sum_{h=1}^H (E_{RES}^h - E_D^h), \quad (9)$$

$$\text{Subject to : } 0 \preceq E_D^h \preceq E_{D,max}, \quad (10)$$

$$0 \preceq E_{RES}^h \preceq E_{RES,max}, \quad (11)$$

$$0 \preceq E_S^h \preceq \max(0, E_{RES}^h - E_D^h). \quad (12)$$

where, E_{RES}^h is prosumer energy generation from renewable energy sources, such as WT or PV array at hour h , E_D^h is prosumer energy demand at hour h and E_S^h is PES at hour h . Stochasticity of base parameters results in multiple ranges of PES defined as:

$$E_S^h = \begin{cases} E_{S,min}^h & \text{for } (E_{D,max}^h \& E_{RES,min}^h) \\ E_{S,mean}^h & \text{for } (E_{D,mean}^h \& E_{RES,mean}^h) \\ E_{S,max}^h & \text{for } (E_{D,min}^h \& E_{RES,max}^h) \end{cases} \quad (13)$$

E. PROSUMER ENERGY COST (PEC)

Stochastic renewable energy sources and prosumer energy demand may result in less prosumers energy generation than prosumers energy demand. At such intervals, prosumers import energy from utility to overcome energy shortage. Prosumers pay for total energy imported from utility known as PEC [35]. An optimization model for PEC is expressed as:

$$\min \sum_{h=1}^H \mathcal{P}^h * (E_D^h - E_{RES}^h), \quad (14)$$

$$\text{Subject to : } 0 \preceq E_D^h \preceq E_{D,max}, \quad (15)$$

$$0 \preceq E_{RES}^h \preceq E_{RES,max}, \quad (16)$$

$$0 \preceq E_C^h \preceq \max(0, \mathcal{P}^h * (E_D^h - E_{RES}^h)). \quad (17)$$

where, \mathcal{P}^h is prosumer energy import rate offered by the smart grid at hour h and E_C^h is PEC at hours h . Stochasticity of base parameters results in multiple ranges of PEC, such as minimum, mean, and maximum PEC defined as:

$$E_C^h = \begin{cases} E_{C,max}^h & \text{for } (E_{D,max}^h \& E_{RES,min}^h) \\ E_{C,mean}^h & \text{for } (E_{D,mean}^h \& E_{RES,mean}^h) \\ E_{C,min}^h & \text{for } (E_{D,min}^h \& E_{RES,max}^h) \end{cases} \quad (18)$$

F. GRID REVENUE (GR)

Bidirectional energy transactions between EDs and utility are fruitful for both prosumers as well as for the smart grid in terms of GR. Prosumers receive benefits in terms

of PES and PEC while an increased GR is generated with a prosumer-based smart grid rather than the conventional power system. The optimization model for GR is presented as:

$$\min \sum_{h=1}^H \mathcal{P}^h * E_U^h + (\mathcal{P}^h - \mathcal{P}_n^h) * E_S^h, \quad (19)$$

$$\text{Subject to : } 0 \leq E_U^h \leq E_{D,max}, \quad (20)$$

$$0 \leq E_S^h \leq E_{RES,max}. \quad (21)$$

where, \mathcal{P}_n^h is the nominal price offered by the smart grid, E_U^h is prosumer energy import from the utility. Stochasticity of base parameters results in multiple ranges of GR, such as minimum, mean, and maximum GR defined as:

$$GR = \begin{cases} GR_{max} & \text{for } (E_{U,max}^h \& \mathcal{P}_{n,min}^h) \\ GR_{mean} & \text{for } (E_{U,mean}^h \& \mathcal{P}_{n,mean}^h) \\ GR_{min} & \text{for } (E_{U,min}^h \& \mathcal{P}_{n,max}^h) \end{cases} \quad (22)$$

The formulae in (13), (18) and (22) are used to represent the ranges that result in the outcomes (PES, PEC, and GR) in different values (ranges from minimum to maximum) depending on the values of prosumer energy demand E_D^h and prosumer energy generation E_{RES}^h .

G. GENETIC ALGORITHM FOR OPTIMIZATION

Genetic Algorithms (GA) are a type of evolutionary algorithms for optimizing both unconstrained and constrained optimization problems [36], [37]. A GA optimizes an objective function (or fitness function) via simulated genetic operators, that is, mutation and crossover. In a GA, a candidate solution is normally encoded by arrays or character of strings to denote chromosomes; however, other representations are also popular [21], [38]–[42]. The GA begins by creating a population of randomly generated solutions; this population is also called the *initial generation*. The GA uses genetic operators to manipulate the solutions from the present generation to produce the next generation of solutions. Crossover is the main genetic operator; it is typically used with a high probability \mathcal{P}_c that ranges from 0.7 to 1.0. The mutation is the other genetic operator, and it flips the values of randomly selected bits (if the chromosome is a bit-string); mutation is employed with a small probability \mathcal{P}_m , usually in the range of 0.001 to 0.05.

To test the quality of the evolving solutions, each solution is evaluated via the fitness function. Moreover, to avoid losing high performing solutions due to genetic operators, GA employs *elitism* whereby a fraction of the best solutions automatically becomes a part of the next generation.

A GA has multiple parameters, each of which can be initialized in different ways. We describe our choices in this paper now. We choose a multi-point crossover that swaps the bits between two solutions at random locations to create a new solution.

The fitness functions of PES, PEC, and GR of the smart grid are defined as:

$$F_S = f(E_{RES}^h, E_D^h), \quad (23)$$

$$F_C = B - f(E_{RES}^h, E_D^h, \mathcal{P}^h), \quad (24)$$

$$F_{GR} = f(E_{RES}^h, E_D^h, \mathcal{P}^h, \mathcal{P}_n^h). \quad (25)$$

where F_S is fitness function as defined in equation (9) for PES is evaluated for pre-managed prosumer load, F_C represents PEC in (14) that is evaluated using pre-managed prosumer load and similarly F_{GR} represents GR objective function given in (19) while B is a large constant to obtain a non-negative fitness function of cost. The objective is to maximize PES and GR and minimize PEC that all achieved using a pre-managed prosumer load. The optimization algorithm for EMM of the prosumer-based smart grid is presented as:

Algorithm 1 Genetic Algorithm Optimization

- 1: **Initialize** with inputs $E_{RES}^h, E_D^h, \mathcal{P}^h$, and \mathcal{P}_n^h .
 - 2: $t = 0$.
 - 3: **Evaluate firstly** $f(E_{RES}^h, E_D^h)$, then $f(E_{RES}^h, E_D^h, \mathcal{P}^h)$, and $f(E_{RES}^h, E_D^h, \mathcal{P}^h, \mathcal{P}_n^h)$ using Eqs. 9-22.
 - 4: **Evaluate** F_S, F_C , and F_{GR} using Eqs. 23-25.
 - 5: **If** F_S, F_C , and F_{GR} converges, **then**,
 - 6: **PES** = $f(E_{RES}^h, E_D^h)$, then **PEC** = $f(E_{RES}^h, E_D^h, \mathcal{P}^h)$, and **GR** = $f(E_{RES}^h, E_D^h, \mathcal{P}^h, \mathcal{P}_n^h)$
 - 7: **Else**
 - 8: $t = t + 1$.
 - 9: **Calculate** next generation individuals $E_{RES}^h, E_D^h, \mathcal{P}^h$, and \mathcal{P}_n^h using Eqs. 9 & 19.
 - 10: **Repeat** steps 3-5.
 - 11: **End**.
-

IV. MACHINE LEARNING (ML) BASED ENERGY MANAGEMENT MODEL (EMM)

ML is a set of techniques enabling software applications to predict future responses of the dependent variables by learning from the training dataset [39]. A given ML method models the inter-relations between covariates and response variables of the training dataset. The training dataset composes of multiple sample points. Generally, the ML algorithms produce more accurate models as the number of sample points increases. Example applications of ML applications include speech recognition, email filtering, image processing, energy and load forecasting, and computer vision. ML uses regression techniques if the output values are numeric, and uses classification techniques if the output values are categorical. Supervised learning with regression best fits in predicting PES, PEC, and GR of the smart grid. In this paper, a GPR model is trained for predicting performance parameters (PES, PEC, and GR) of EMM.

A. TRAINING AND TEST DATA DESCRIPTION

Training data contains input covariates (prosumer available energy, load, and pricing) and response variables (PES, PEC, GR). Copano Bay and Brownsville Texas US with enough wind and solar potentials are considered as operational zones for energy generation and bidirectional energy trade between EDs and utility under SA-SLA. Hourly data is collected from trustful sources [43] and used to compute training covariates while the data set for ML model training is generated using the collected hourly data and response variable that is generated from the optimization scheme. Stochasticity of WS, SI, and prosumers load profile results in dynamic covariates. As ML algorithms require all possible dynamics and scenarios of training data for entire learning, a complete set of test covariates are computed by repetitive measures of covariates using stochastic source parameters. Statistics and ML Toolbox of MATLAB are used to train the GPR Matern 5/2 model and PES, PEC, and GR are obtained as a test response variable from the trained model. Results of ML and optimization schemes i.e. GA and PSO (also consider for a fair comparison) are compared for seasonal variations, and different statistical tests are performed to prove the validity of our proposed ML learning approach to predict the performance matrix.

B. GAUSSIAN PROCESS REGRESSION (GPR) BASED EMM

GPR also is known as kriging is a nonlinear interpolation method that predicts responses by the Gaussian process based on preceding covariances. The Gaussian process is a method of statistics theory in which a finite collection of stochastic variables distributed in multiple time slots follows a multivariate gaussian distribution. Training data $T = \{(x_i, y_i) | i = 1, 2, \dots, m\}$ is given as the input to regression learning, where x denotes covariates (renewable energy sources, load, price), y represents outputs (PES, PEC, GR), and m indicates the number of observations. In the generalized model, covariates include one or more independent variables belonging to \mathbb{R}/\mathbb{R}^n , where n is the number of independent variables, result in one or more dependent variables based on the nature of the problem. In the proposed work, the GPR model is trained by $T = \{(x_{ij}, y_{ij}) | i = 1, 2, \dots, 31; j = 1, 2, 3\}$ as the training dataset, where $x_{i1} \in \mathbb{R}^2 (E_{RES}^h, E_D^h)$, $x_{i2} \in \mathbb{R}^3 (E_{RES}^h, E_D^h, \mathcal{P}^h)$, and $x_{i3} \in \mathbb{R}^4 (E_{RES}^h, E_D^h, \mathcal{P}^h, \mathcal{P}_n^h)$ for output $y_{i1} \in \mathbb{R}$ (PES), $y_{i2} \in \mathbb{R}$ (PEC), and $y_{i3} \in \mathbb{R}$ (GR) respectively. Trained model takes x_{test} as an input test covariate and produce y_{test} as a predicted response. Generalized GPR model used to predict the required output from a set of inputs covariates is defined as:

$$y = h(x)^T \beta + f(x), \quad f(x) \sim GP(0, k(x, x')), \quad (26)$$

where latent function $f(x)$ represents the Gaussian process based on covariance $k(x, x')$ of covariates $(E_{RES}^h, E_D^h, \mathcal{P}^h, \mathcal{P}_n^h)$, $h(x)^T$ denotes explicit basis function of covariates $(E_{RES}^h, E_D^h, \mathcal{P}^h, \mathcal{P}_n^h)$, and β represents the coefficient of training covariates $(E_{RES}^h, E_D^h, \mathcal{P}^h, \mathcal{P}_n^h)$. The Gaussian process with zero mean

and identical distribution is assumed here. GPR most fits our case and provides the best results as the data approximately follow the Gaussian process. Covariance free parameters are regarded as hyperparameters. Known hyperparameters serve as a base assumption to make an inference. At any instant, the output y from predictive GPR model for training dataset is defined as:

$$P(y_i | f(x_i), x_i) \sim \mathcal{N}(y_i | h(x_i)^T \beta + f(x_i), \sigma^2), \quad (27)$$

where σ is standard deviation and σ^2 is the variance of input covariates. The prosumer energy generation through renewable energy sources given in Eq. 11 is taken as:

$$P(Y | f, X) \sim \mathcal{N}(Y | H\beta + f, \sigma^2 I), \quad (28)$$

Statistic and ML Toolbox is used to train given the GPR model by training dataset. Variance is designated as $69.43e^{+3}$ and the value of β is calculated as $1.0463e^{+5}$. Kernel function associated with GPR Matern 5/2 is expressed as:

$$k(x_i, x_j) = \sigma_E^2 \left(1 + \frac{\sqrt{5}r}{\sigma_E} + \frac{5r^2}{r\sigma_E^2} \right) \exp\left(-\frac{\sqrt{5}r}{\sigma_E}\right), \quad (29)$$

where, $r = \sqrt{((x_i - x_j)^T (x_i - x_j))}$ is Euclidean distance between two adjacent input covariates x_i and x_j .

V. PERFORMANCE EVALUATION

A. DATA ANALYSIS

Hourly data collected from the national renewable electrical laboratory is considered for analysis of EMM. Useful statistic of the data is collected using average values for simulation scenarios. An averages data set for different seasons of the ten years, namely spring season, summer season, winter season, and the fall season is considered. ED1 and ED2 are considered for simulations at Copano Bay Texas US with longitude and latitude coordinates of -97.0 and 28.1 respectively while ED3 is considered for simulations at Brownsville Texas US with longitude and latitude coordinates of -97.5 and 25.9 respectively. For simulation analysis, installation of WT at Copano bay and PV arrays at Brownsville Texas US is considered due to the following potential reasons, namely: (a) enough solar potential of Brownsville can be utilized for massive energy production, (b) significant wind potential of Copano Bay can be utilized to generate abundant energy.

B. SEASONAL VARIATIONS OF EMM PARAMETERS

Seasonal variations affect energy consumption and energy production pattern of EDs prosumers because of different environmental shifts throughout a year. Energy consumption and energy production dynamics of prosumers greatly influenced the shaping of performance parameters (PES, PEC, and GR) of EMM. In this context, four seasons of the year, namely spring season, summer season, fall season, and winter season are considered for the design and analysis of EMM.

1) SPRING SEASON AT DATA ANALYSIS

Spring season is from March to May at Copano Bay and Brownsville Texas US. Optimization (GA and PSO) and ML (GPR) based PES, PEC, and GR of spring season calculated using Algorithm 1 and (26-29) are depicted in Figures 3-5 respectively. The vertical axis of Figures 3-5 are labeled with PES (in MWhr), PEC (in \$/MWhr), and GR (in \$/MWhr) while the horizontal axis is labeled with time (in days of March). The red lines with hexagons represent ML-based PES, PEC, and GR while the plane blue line represents GA Optimization based PES, PEC, and GR. The dark dashed line shows Particle Swarm Optimization (PSO) based PES, PEC, and GR and straight yellow line at the top is the maximum energy-producing capacity of prosumers. The performance of ML-based PES and GA and PSO-based PES are comparable as shown in Figure 3. ML performs better than both GA and PSO optimization techniques on the 20th day while GA optimization performs well than ML and PSO on the 25th day. Similarly, PEC of spring, calculated using optimization (GA and PSO) and ML (GPR) is shown in Figure 4. The performance of ML-based PEC and GA optimization-based PEC is comparable. On the 20th day, ML shows high performance while GA optimization performs well on the 25th day. The lowest possible PEC achieved is through ML and performs better with decreased PEC. GR of spring season calculated using optimization (GA and PSO) and ML (GPR) is depicted in Figure 5. GA Optimization outperforms ML and PSO on 3rd day while the high performance of ML is recorded on the 10th day. Highest GR is achieved through GA optimization, but on average ML performs better.

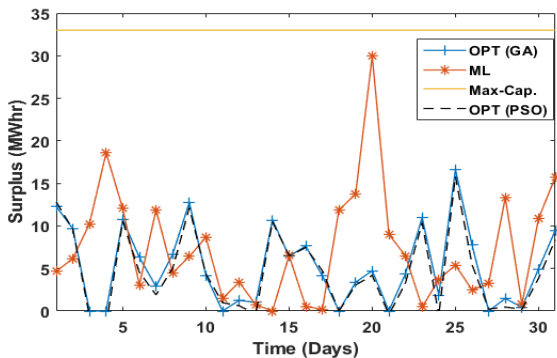


FIGURE 3. Optimized and machine learning based prosumer energy surplus of spring season.

2) SUMMER SEASON AT DATA ANALYSIS

Summer season is from June to September at Copano Bay and Brownsville Texas US. Optimization (GA and PSO) and ML (GPR) based PES, PEC, and GR of summer season calculated using Algorithm 1 and (26-29) are depicted in Figures 6-8 respectively. The vertical axis of Figures 6-8 are labeled with PES (in MWhr), PEC (in \$/MWhr), and GR (in \$/MWhr) while the horizontal axis is labeled with time (in days of June). The red line with hexagons represents

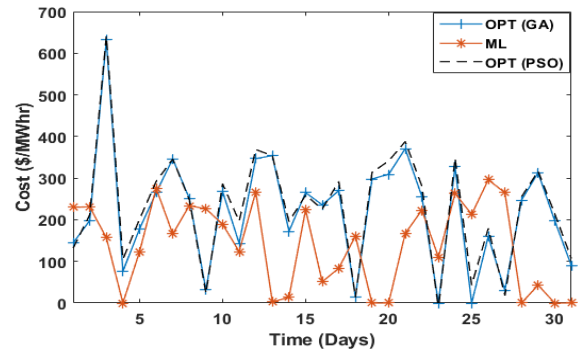


FIGURE 4. Optimized and machine learning based prosumer energy cost of spring season.

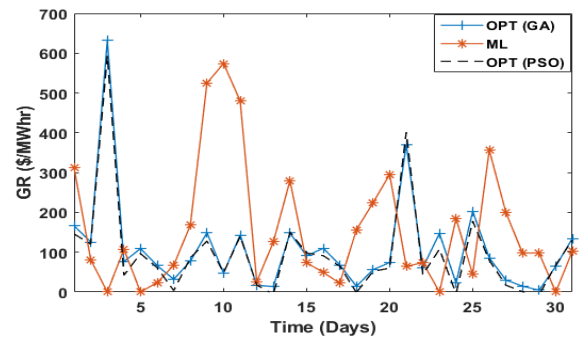


FIGURE 5. Optimized and machine learning based grid revenue. GR: grid revenue of spring season.

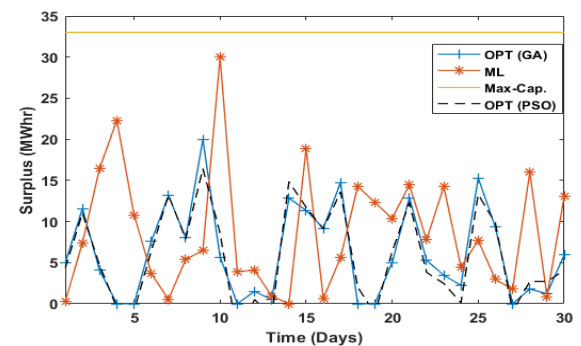


FIGURE 6. Optimized and machine learning based prosumer energy surplus of summer season.

ML-based PES, PEC, and GR while the plane blue line represents GA optimization-based PES, PEC, and GR. The dark dashed line represents PSO-based PES, PEC, and GR while a yellow straight line at the top is maximum energy producing capacity of prosumers. The stochasticity of environmental parameters causes different PES of optimization and ML. ML performance is experienced better in terms of PES as shown in Figure 6.

PEC of the summer season calculated using optimization techniques (GA and PSO) and ML is presented in Figure 7. GA optimization outperforms ML in terms of PEC on the 26th day while ML results in decreased PEC on the 19th day. Similarly, GR of smart grid generated using optimization, and

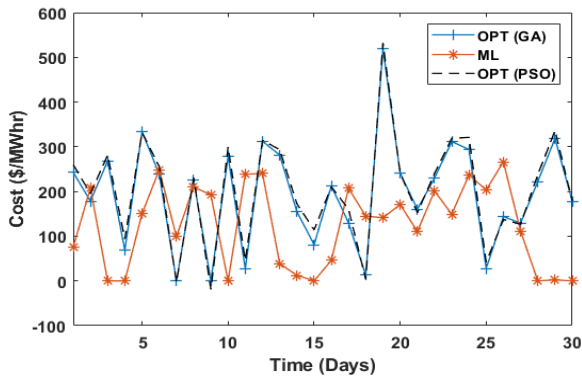


FIGURE 7. Optimized and machine learning based prosumer energy cost of summer season.

ML is depicted in Figure 8. GA optimization outperforms ML and PSO on the 19th day while ML outperforms GA and PSO on the 20th day in terms of GR. Overall, better performance of ML is noticed in the summer season.

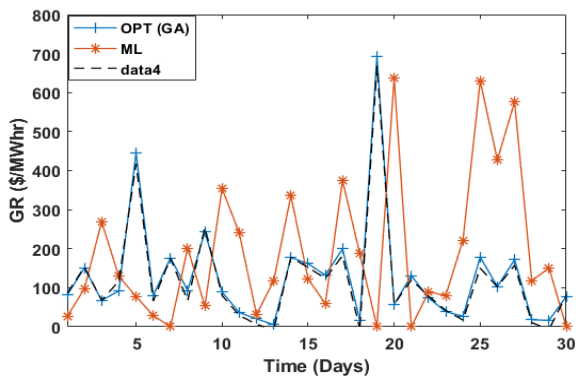


FIGURE 8. Optimized and machine learning based grid revenue of summer season.

3) WINTER SEASON AT DATA ANALYSIS

Winter season is from December to February at Copano Bay and Brownsville Texas US. Winter is accompanied by more wind blowing but less sunny days. So, an average energy generation by WT and PV arrays is possible in the winter season. Optimization (GA) and ML (GPR) based PES, PEC, and GR of winter season calculated using Algorithm 1 and (26-29) are depicted in Figures 9-11 respectively. The vertical axis of Figures 9-11 are labeled with PES (in MWhr), PEC (in \$/MWhr), and GR (in \$/MWhr) while the horizontal axis is labeled with time (in days of December). Different PES is associated with optimization (GA and PSO) and ML because of the stochasticity of environmental parameters. ML outperforms optimization (GA and PSO) on 4th day while GA optimization outperforms ML on 25th day in terms of PES as shown in Figure 9. Performances of optimization and ML are comparable but overall better ML performance is experienced in terms of PES. PEC of the winter season calculated using optimization (GA and PSO) and ML is

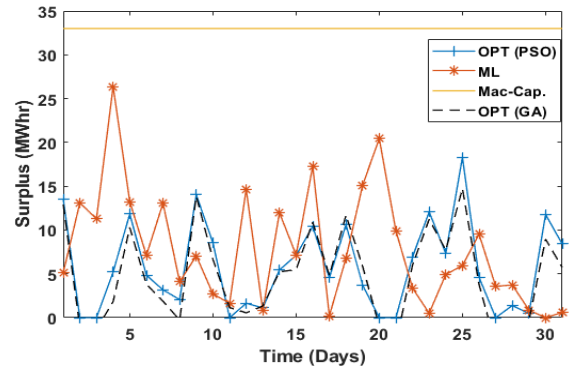


FIGURE 9. Optimized and machine learning based PES of winter season.

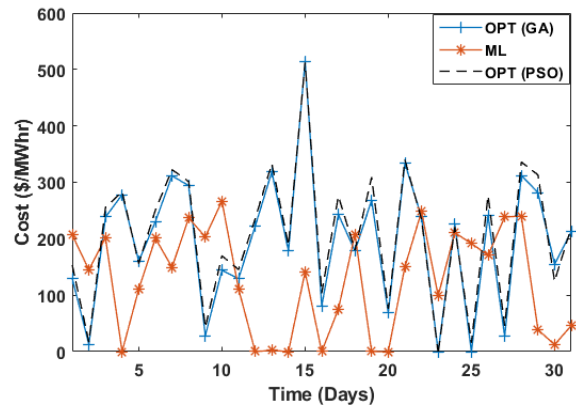


FIGURE 10. Optimized and machine learning based prosumer energy cost of winter season.

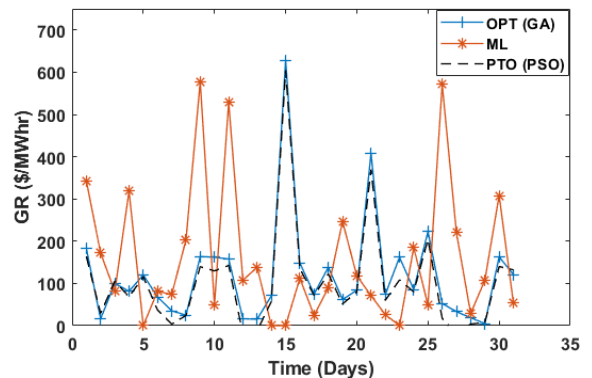


FIGURE 11. Optimized and machine learning based grid revenue of winter season.

presented in Figure 10. Optimization outperforms ML on the 10th day while ML outperforms optimization on the 15th day in terms of PEC. Similarly, GR of the smart grid, generated using optimization, and ML are depicted in Figure 11. GA optimization outperforms ML on the 15th day while ML outperforms optimization on the 26th day in terms of GR. Overall, better performance of ML is noticed in the winter season.

4) FALL SEASON AT DATA ANALYSIS

The fall season is observed from October to November at Copano Bay and Brownsville Texas US. Optimization (GA and PSO) and ML (GPR) based PES, PEC, and GR of fall season calculated using Algorithm 1 and (26-29) are depicted in Figures 12-14 respectively. The vertical axis of Figures 12-14 are labeled with PES (in MWhr), PEC (in \$/MWhr), and GR (in \$/MWhr) while the horizontal axis is labeled with time (in days of October). The red lines with hexagons represent ML-based PES, PEC, and GR while the plane blue line represents GA Optimization based PES, PEC, and GR. The dark dashed line shows Particle Swarm Optimization (PSO) based PES, PEC, and GR and straight yellow line at the top is the maximum energy-producing capacity of prosumers. The performance of ML-based PES and GA and PSO-based PES are comparable as shown in Figure 12.

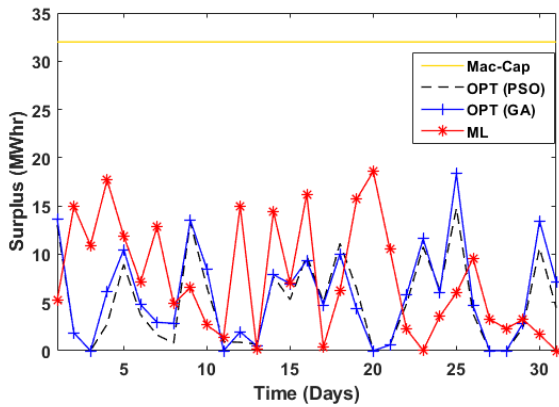


FIGURE 12. Optimized and machine learning based PES of fall season.

ML performs better than both GA and PSO optimization techniques on the 4th and 20th day of October while GA optimization performs well than ML and PSO on the 25th day of October. Similarly, PEC of spring, calculated using optimization (GA and PSO) and ML (GPR) is shown in Figure 13. The performance of ML-based PEC and GA optimization-based PEC is comparable. On the 20th day, ML shows high performance while GA optimization performs well on the 25th day. The lowest possible PEC achieved is through ML and performs better with decreased PEC. GR of spring season calculated using optimization (GA and PSO) and ML (GPR) is depicted in Figure 14. GA Optimization outperforms ML and PSO on the 25th day while the high performance of ML is recorded on the 9th day. Highest GR is achieved through GA optimization, but on average ML performs better.

C. SERVICE LEVEL AGREEMENT (SLA) ANALYSIS

Optimization and ML-based SLAs of the spring season are depicted in Figures 15 and 16. The horizontal axis of Figures 15 and 16 are labeled with PES (in MWhr) while the vertical axis is labeled with PEC (in \$/MWhr). In Figure 15 and Figure 16, an area surrounded by a red line represents ROC of SLA1 while the areas surrounded

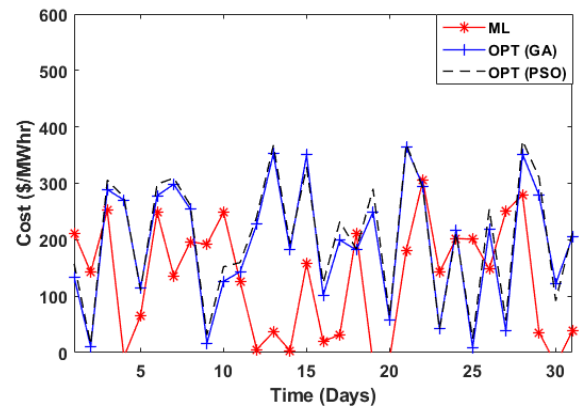


FIGURE 13. Optimized and machine learning based PEC of fall season.

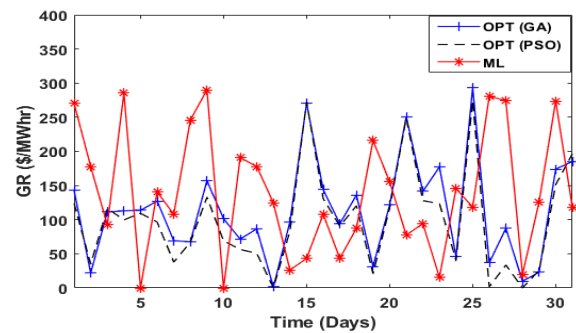


FIGURE 14. Optimized and machine learning based GR of fall season.

by blue and black lines represent ROC of SLA2 and SLA3 respectively.

It is noticed from Figure 15 that PEC decreases as we move down from SLA1 to SLA3 because of higher contracted PES of SLA3. Similarly, it is noticed from Figure 16 that PEC decreases as we move down from SLA1 to SLA3 because of higher contracted PES of SLA3. Moreover, the analysis of Figure 15 and Figure 16 reveal that ML-based multiple smart SLAs are wider with less PEC. It is concluded that, for the same PES, prosumers are liable to pay less PEC by ML approach and so, receive more benefits.

Optimization and ML-based SLAs of the summer season are depicted in Figures 17 and 18. The horizontal axes of Figures 17 and 18 are labeled with PES (in MWhr) while the vertical axis is labeled with PEC (in \$/MWhr). In Figure 17 and Figure 18, an area surrounded by a red line represents ROC of SLA1 while the areas surrounded by blue and black lines represent ROC of SLA2 and SLA3 respectively. It is noticed from Figure 17 that PEC decreases as a move down from SLA1 to SLA3 because of higher contracted PES of SLA3. Similarly, it is noticed from Figure 18 that PEC decreases as we move down from SLA1 to SLA3 because of higher contracted PES of SLA3. Moreover, the analysis of Figure 17 and Figure 18 reveal that the ROC of ML-based SLA becomes wider and shrinks to the bottom portion of the graph with less PEC. It is concluded that, for the same PES,

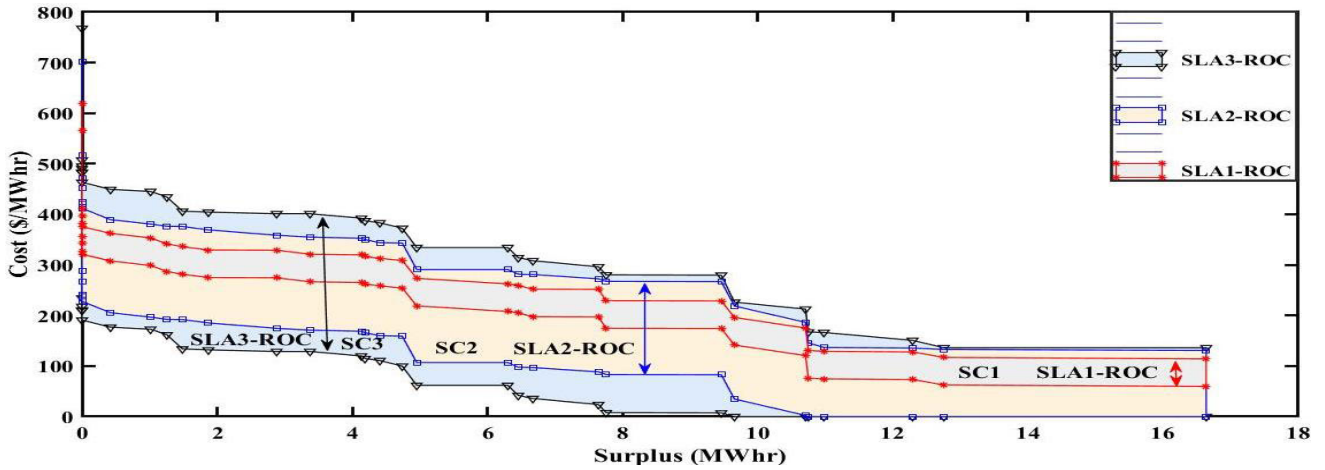


FIGURE 15. Optimization based SLA for the spring season.

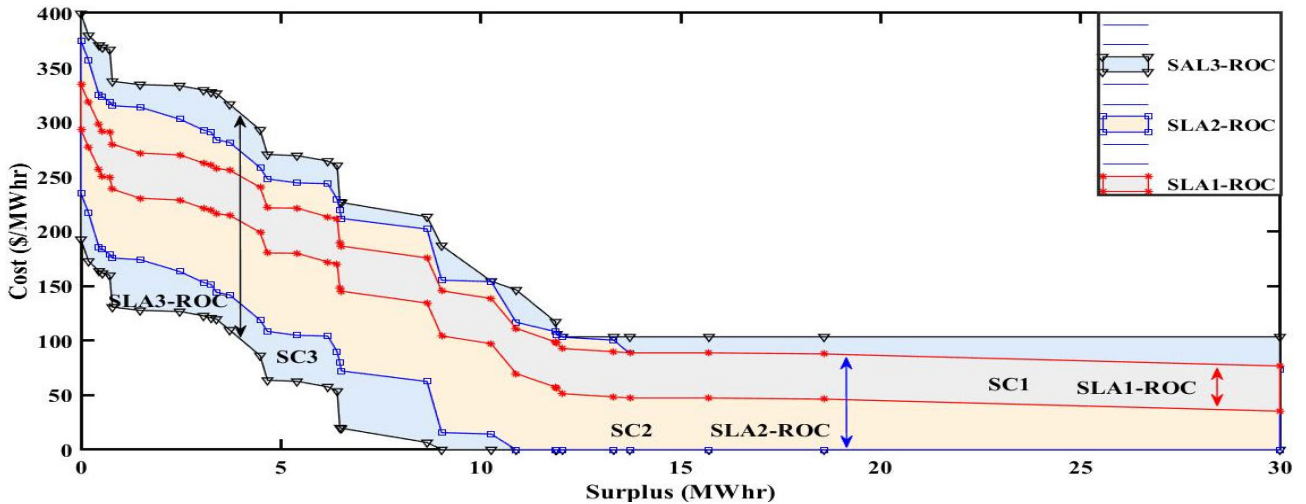


FIGURE 16. Machine learning based SLA for the spring season.

prosumers are liable to pay less PEC by ML approach. So, more benefits are associated with the ML approach in terms of decreasing PEC in the summer season.

Optimization and ML-based SLAs of the winter season are depicted in Figures 19 and 20. The horizontal axis of Figures 19 and 20 are labeled with PES (in MWhr) while the vertical axis is labeled with PEC (in \$/MWhr). In Figure 19 and Figure 20, an area surrounded by a red line represents ROC of SLA1 while the areas surrounded by blue and black lines represent ROC of SLA2 and SLA3 respectively.

It is noticed from Figure 19 that PEC decreases as we move down from SLA1 to SLA3 because of higher contracted PES of SLA3. Similarly, it is noticed from Figure 20 that PEC decreases as we move down from SLA1 to SLA3 because of higher contracted PES of SLA3. Analysis of Figure 19 and Figure 20 reveals that the ROC of ML-based SLA becomes wider and shrinks to the bottom portion of the graph with

less PEC. It is also noticeable that the uppermost PEC is less for ML-based SLA. It is concluded that ML outperforms optimization as for the same PES, less PEC is associated with ML-based SLA. So, more benefits are associated in the winter season with the ML approach in terms of decreasing PEC.

D. CONVERGENT AND DIVERGENT LIMITS OF SLAs

Convergence and divergence limits provide sense about the region of benefits for stakeholders. That is why it is important to know about convergent and divergent limits of SLA. PES and PEC are approximately normally distributed because of their dependence on normally distributed renewable energy as described by the following subsection. So, 95% area under the probability density curve of PES, PEC, and GR is taken as convergence region for SLA while the outer 5% area is taken as a region of divergence for SLA. Complete numeric detail about ROC and ROD of PES, PEC, and GR is provided in the tabular analysis section of this paper.

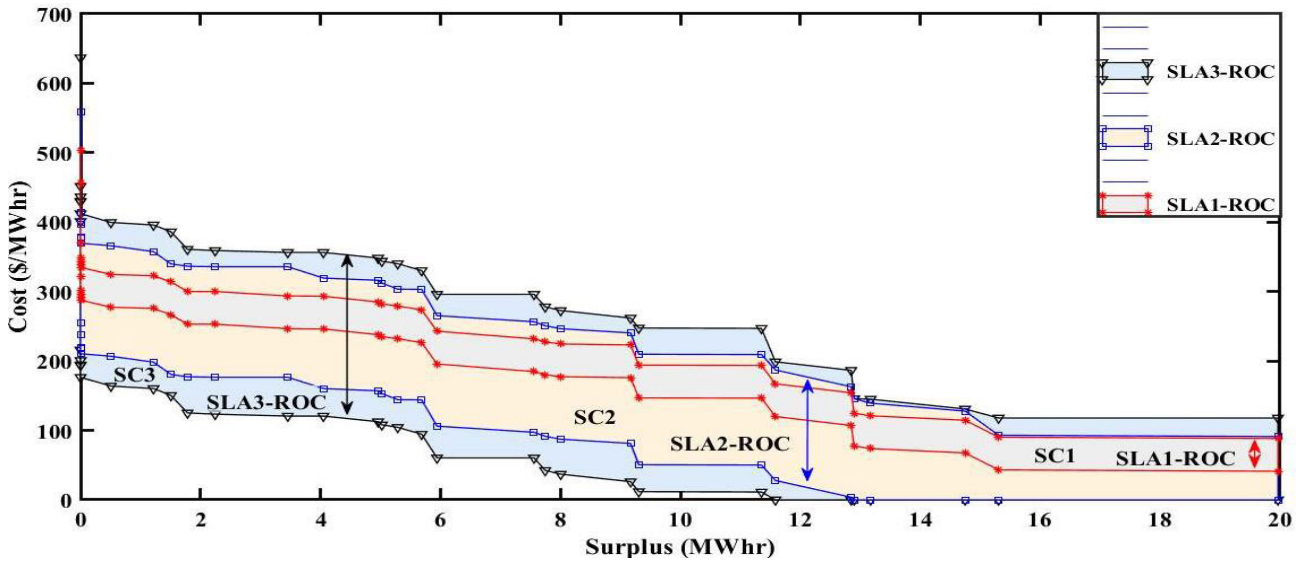


FIGURE 17. Optimization based SLA for the summer season.

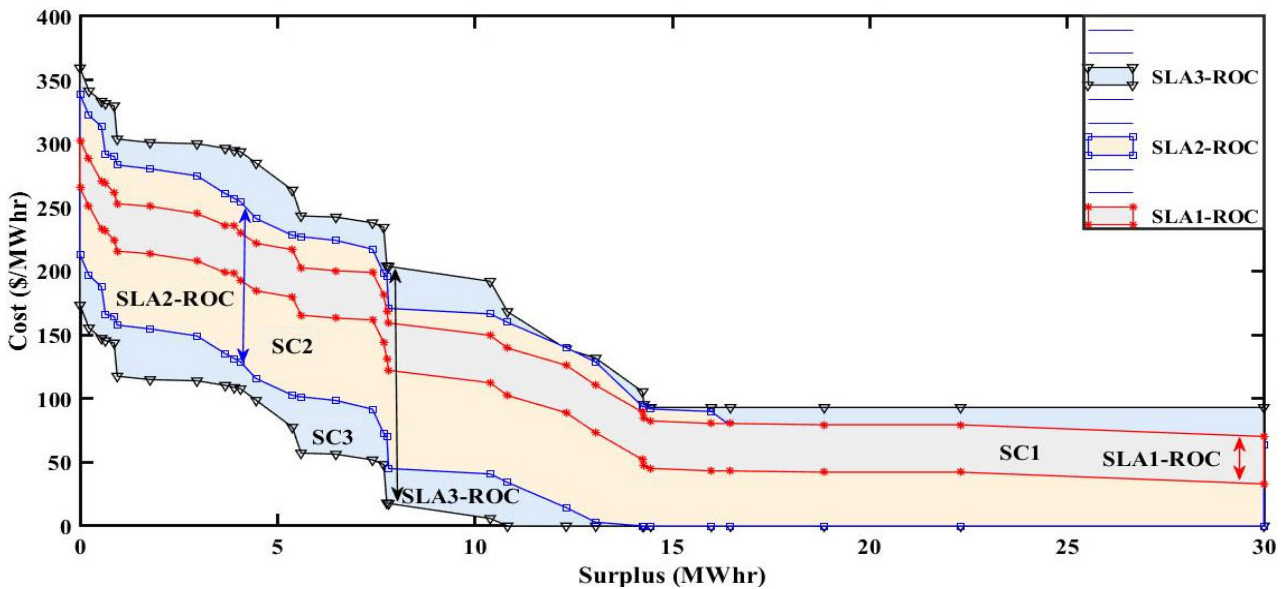


FIGURE 18. Machine learning based SLA for the summer season.

E. STATISTICAL ANALYSIS

Statistical tests are the best tool to describe different data characteristics. The statistical analysis develops knowledge about five important information, such as describes the nature of data under analysis, explores different underlying characteristics of data, prove or disprove the validity of the model to be analyzed, and develops an understanding about future action. Keeping in view the importance of statistical tests, multiple tests are performed, described in subheadings below.

1) NORMAL QUANTILE-QUANTILE (Q-Q) PLOTS

The plot between the observed and expected value of a specific data set is named as the Q-Q plot. Q-Q plots describe

the nature (distribution) of data. Q-Q plots are of different types to show whether considered data follow the specific distribution or not. Normal Q-Q plots are presented and examined in this paper as the best fit for our scenario with normally distributed energy generation through renewable energy sources. The Q-Q plots of PES, PEC, and GR are presented in Figures 21-23 respectively. The horizontal axis of Figure 21 is labeled with standard normal values of the normal distribution curve while the vertical axis represents PES (in MWhr). The straight inclined red line represents the perfect normal line. Small circles close to and symmetric around the perfect normal line, reveals that PES is approximately normal in both cases (optimization and ML).

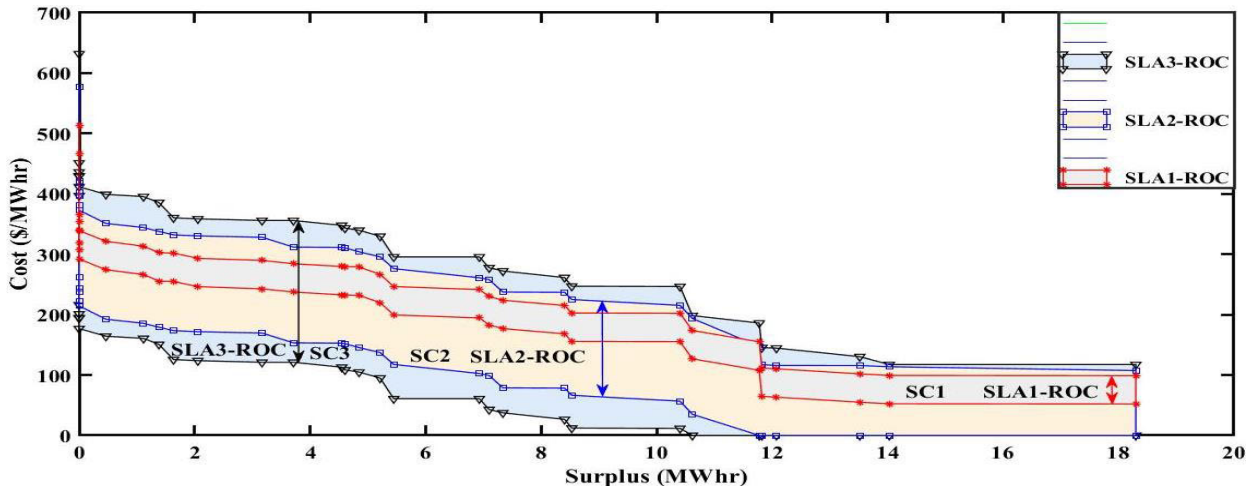


FIGURE 19. Optimization based SLA for the winter season.

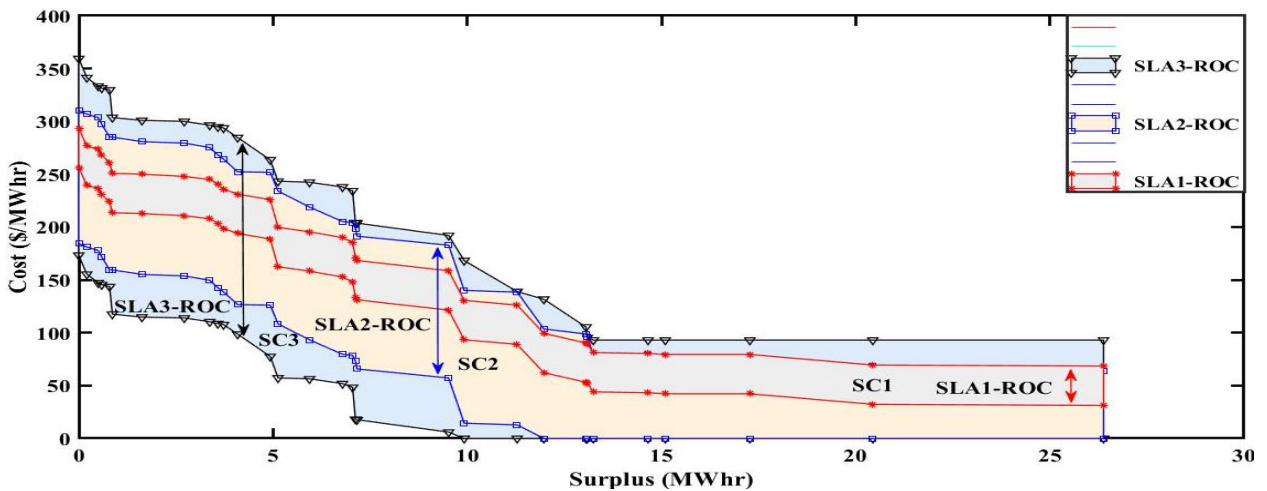


FIGURE 20. Machine learning based SLA for the winter season.

Similarly, the horizontal axis of Figure 22 is labeled with standard normal values of the normal distribution curve while the vertical axis represents PEC (in \$/MWhr). Small circles close to and symmetric around the perfect normal line, reveals that PEC is approximately normal in both cases (optimization and ML). The horizontal axis of Figure 23 is labeled with standard normal values of the normal distribution curve while the vertical axis represents GR (in \$/MWhr). Small circles close to and symmetric around the perfect normal line, reveals that GR is approximately normal in both cases (optimization and ML). PES, PEC, and GR of the smart grid are experienced to follow approximate normal distribution which proves the validity of ML-based EMM in estimating PES, PEC, and GR.

2) BOX PLOTS

Box plot reveals important information by providing the lowest observation, lower quartile, median, upper quartile, highest observation, and outliers of the given data set. Box plot

of PES, for the spring season, is presented in Figure 24. The vertical axis of Figure 24 represents PES (in MWhr) while the horizontal axis represents optimized and ML categories of PES for all three EDs. It is noticeable that higher PES of EDs is associated with ML. Similarly, the box plot of PEC, for the spring season is presented in Figure 25. The vertical axis of Figure 25 represents PEC (in \$/MWhr) while the horizontal axis represents optimized and ML categories of PEC for all three EDs. Figure 25 depicts that reduced PEC of EDs is associated with ML. Box plot representation of GR of the smart grid for the spring season is presented in Figure 26. The vertical axis of Figure 26 represents GR (in \$/MWhr) while the horizontal axis represents optimized and ML categories of GR for all three EDs. Figure 26 depicts that reduced PEC of EDs is associated with ML. Less PEC, more PES, and more GR of the spring season, associated with the ML approach prove the validity of our proposed ML-based EMM.

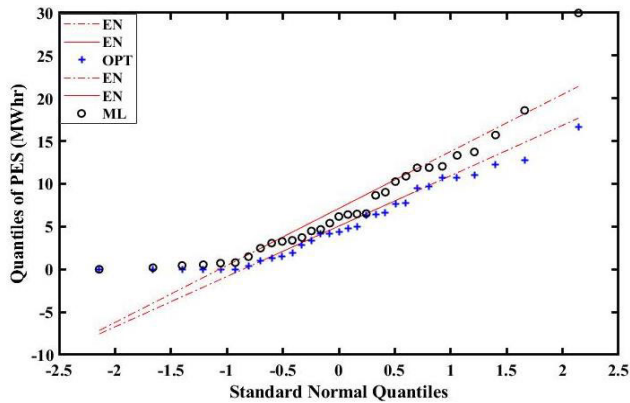


FIGURE 21. Normal Q-Q plot of optimization and machine learning based prosumer energy surplus. EN: Exact Normal, OPT: Optimization, ML: Machine Learning.

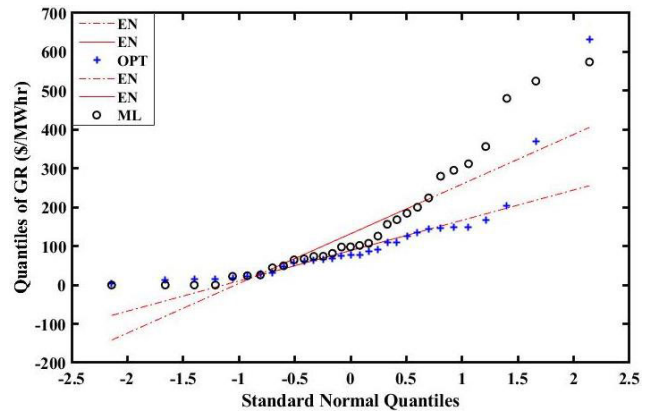


FIGURE 23. Normal Q-Q plot of Optimization and Machine Learning based Grid Revenue. EN: Exact Normal, OPT: Optimization, ML: Machine Learning.

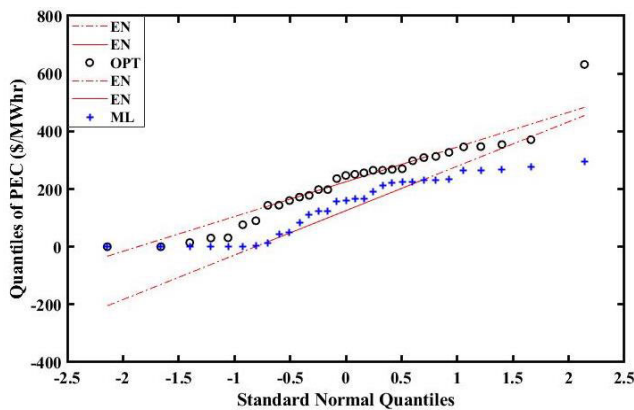


FIGURE 22. Normal Q-Q plot of optimization and machine learning based prosumer energy cost. EN: Exact Normal, OPT: Optimization, ML: Machine Learning.

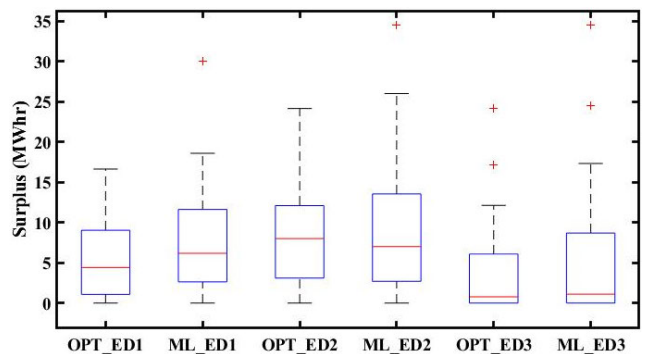


FIGURE 24. Box plots of optimization and machine learning based prosumer energy surplus for the spring season.

Box plot of PES, for the summer season, is presented in Figure 27. The vertical axis of Figure 27 represents PES (in MWhr) while the horizontal axis represents optimized (GA and PSO) and ML categories of PES for all three EDs. It is noticeable that higher PES of EDs is associated with ML. Similarly, the box plot of PEC, for the summer season is presented in Figure 28. The vertical axis of Figure 28 represents PEC (in \$/MWhr) while the horizontal axis represents optimized (GA and PSO) and ML categories of PEC for all three EDs. Figure 28 depicts that reduced PEC of EDs is associated with ML. Box plot representation of GR of the smart grid for the summer season is presented in Figure 29. The vertical axis of Figure 29 represents GR (in \$/MWhr) while the horizontal axis represents optimized (GA and PSO) and ML categories of GR for all three EDs. Figure 29 depicts that reduced PEC of EDs is associated with ML. Less PEC, more PES, and more GR of the summer season, associated with the ML approach prove the validity of our proposed ML-based EMM.

F. TABULAR ANALYSIS

It is important to exactly know the convergence and divergence limits of optimization and ML-based SLA for all

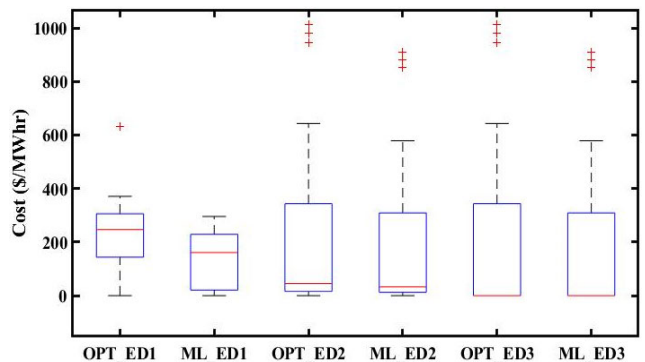


FIGURE 25. Box plots of optimization and machine learning based prosumer energy cost for the spring season.

three EDs. To obtain stakeholders mutual benefits, PES, PEC, and GR must lie in the corresponding convergence region. The spring, summer, and winter contractual limits of optimization (GA and PSO) and ML-based PES, PEC, and GR for all three EDs are tabulated in Table 1. From Table 1, it is concluded that more PES, less PEC, and more GR is associated with the ML approach of designing EMM and increase the mutual benefits of stakeholders.

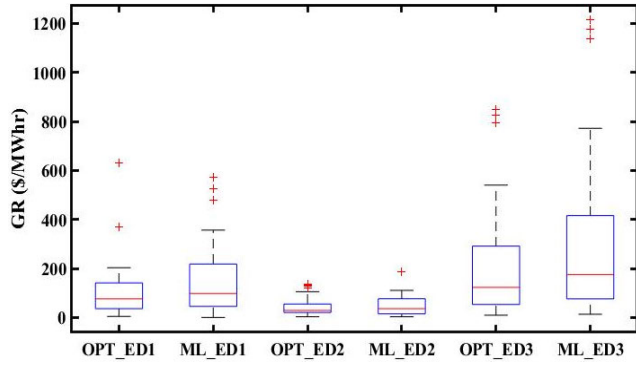


FIGURE 26. Box plots of optimization and machine learning based grid revenue for the spring season. OPT: Optimization, ML: Machine Learning.

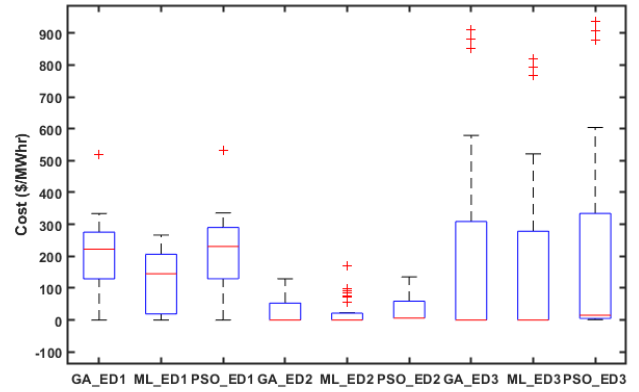


FIGURE 28. Box plots of optimization and machine learning based prosumer energy cost for the summer season.

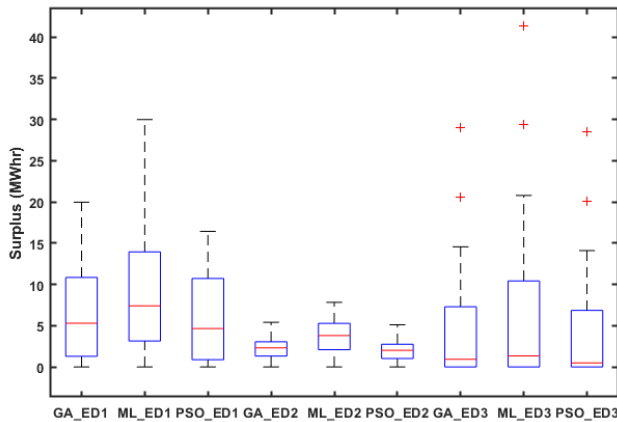


FIGURE 27. Box plots of optimization and machine learning based prosumer energy surplus for the summer season.

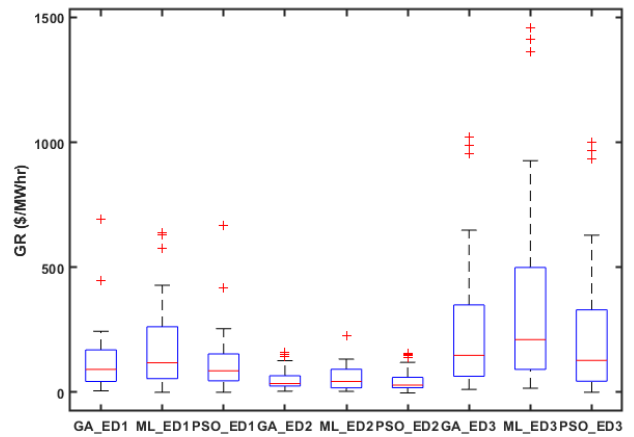


FIGURE 29. Box plots of optimization and machine learning based grid revenue for the summer season.

G. CRITICAL DEBATE

EDs prosumers generate energy using WT and PV arrays. Stochasticity of environmental parameters results in variable energy generation of prosumers and produces end effect on PES, PEC, and GR. The optimization techniques being used from the past few decades are robust to work in such type of stochastic environment and produces the best results. However, the accuracy of the optimization process depends on the known variation expected in the system in the form of training data in hand, and the optimization algorithm finds the minimum/ maximum value to the best solution of the problem. If the system has unknown variations or the data for the training do not capture all constraints variation, then comes the advantage of ML that works on the generalization of the data that we do not have. Therefore, ML works and produces outcomes by learning from previous data interrelations. This makes ML easy to work than optimization. As the performance of ML algorithms is affected by some sample points, it requires all types of sample points for complete learning. If a machine is made to learn from an incomplete set of samples, ML results in useless outcomes when untrained test data is provided. Figures 3-14 depict that ML competes with

optimization in estimating response parameters (PES, PEC, and GR) of EMM.

The stochasticity of environmental parameters creates variability in prosumer energy generation. The stochasticity of prosumers energy generation results in multiple ranges of PES. Multiple SCs with small variations of PES are developed instead of fixed contracts with large variability of PES in response to stochastically changing PES. In this respect, optimized multiple SCs based SA-SLA incorporating stochasticity of environmental parameters (wind speed and solar irradiance), multiple SCs, and smart SLAs are developed as depicted in Figure 15, Figure 17, and Figure 19.

Each of smart SLAs associates it's ROC based on SCs. PEC increases as we move down from SLA3 to SLA1 because of the decreasing slope of contracted PES from SLA3 to SLA1. Similarly, ML-based multiple smart SLAs of Figures 16, 18, and 20 depict the same pattern as of optimization-based on multiple smart SLAs of Figures 15, 17, and 19. The above discussion of SA-SLA clears that multiple smart SLAs based on multiple SCs with small variations in contractual values of PES is more beneficial to stakeholders. Moreover, critical analysis of multiple SCs based smart SLAs of Figures 15-20

TABLE 1. Region of convergence of pes, PEC, and GR for spring, summer, and winter season using ml and optimization (ga and pso).

EDs	Seasons	Approach	ROC of PES	ROC of PEC	ROC of GR
ED1	Spring	OPT (GA)	9.8800-2.2037	355.27-105.74	230.06-32.325
		OPT (PSO)	8.9823-2.4827	383.21-113.83	212.31-36.825
		ML	13.889- 2.8005	243.35-67.018	312.84-60.229
	Summer	OPT (GA)	11.856-2.6444	313.38-97.258	264.67-39.650
		OPT (PSO)	10.3826-3.1927	358-91-95.531	254.39-41.273
		ML	15.833-3.4663	219.02-60.317	369.21-72.264
	Winter	OPT (GA)	10.868-2.4240	312.83-97.430	243.03-36.951
		OPT (PSO)	10.2835-2.8726	343.74-91-725	240.28-37.837
		ML	14.373-3.1966	219.02-60.316	320.20-59.659
ED2	Spring	OPT (GA)	15.457-3.1266	533.21-93.774	84.340-16.638
		OPT (PSO)	13.0273-2.9735	545.42-89.261	79.736-19.927
		ML	16.140-3.6311	479.30-84.127	89.128-18.469
	Summer	OPT (GA)	3.6619-1.0818	75.377-14.196	101.21-19.966
		OPT (PSO)	3.3709-1.2938	89.238-13.982	93.292-20.273
		ML	5.8869-1.8317	64.891-11.430	106.95-22.163
	Winter	OPT (GA)	3.7626-1.2182	75.377-14.196	93.209-18.445
		OPT (PSO)	2.7194-1.4925	79.382-14.271	91.283-21.726
		ML	6.2267-1.8365	49.799-9.2247	96.911-19.772
ED3	Spring	OPT (GA)	9.6747-1.5675	529.55-91.744	468.35-85.693
		OPT (PSO)	8.8231-1.2834	538.83-90.872	451.72-91.283
		ML	13.821-2.2392	476.60-82.569	669.07-122.42
	Summer	OPT (GA)	11.610-1.8810	477.70-83.785	562.01-102.83
		OPT (PSO)	11.2735-1.9263	491.26-84.938	551.83-112.63
		ML	16.5851-2.6871	428.94-74.312	802.88-146.90
	Winter	OPT (GA)	3.7626-1.2182	75.377-14.196	93.209-18.445
		OPT (PSO)	3.5936-1.8273	79.271-13.272	91.287-19.273
		ML	6.2267-1.8365	49.799-9.2247	96.911-19.772

clear the point of our interest that for the same PES, decreased PEC is associated with ML approach.

Statistical Analysis and tabular comparison for spring, summer, and winter seasons of the year are performed to statistically show the performance of the ML approach. The Q-Q plots of Figures 21-23 prove the validity of the ML approach by representing that outcomes of ML follow approximate Gaussian distribution as optimization outcomes follow. The box plots of Figures 24-32 represent that the ML approach is associated with increased PES, decreased PEC, and increased GR of spring, summer, and winter season for all three EDs. Moreover, statistics of Table 1 clarify that

ML outcomes are improved in terms of SLA convergence regions of spring, summer, and winter seasons for all three EDs. Advantages and disadvantages are associated with both optimization and ML, but the purpose of this document is clear that ML can be used to design an EMM within the smart grid.

H. COMPUTATIONAL COMPLEXITY

ML training is offline computationally expensive processing that consumes less computational time with online implementation of the trained model in comparison with online optimization models. For real-time implementation,

the ML model requires input or output processing without involving the training process. In the case of massive stochasticity or emergency burden, the complex data set can further be computed through fast processing GPU data centers based on Amazon EC2 Criterion.

VI. CONCLUSION AND FUTURE WORK

To conclude, predicted responses of ML-based EMM are compared with outcomes of Optimization-based EMM in terms of PES, PEC, and GR. Results show that ML-based EMM competes with Optimization-based EMM and outperforms in computing optimized EMM parameters. In the spring season, ML-based EMM results in 29% more PES, 46% less PEC, and 27% more GR for ED1 while 5% more PES, 11% less PEC, and 6% more GR for ED2 and 30% more PES, 11% less PEC, and 31% more GR for ED3. In the summer season, ML-based EMM results in 26% increased PES, 42% decreased PEC, and 33% increased GR for ED1 while 38% more PES, 17% less PEC, and 5% more GR for ED2 and 31% more PES, 11% less PEC, and 30% more GR for ED3. Similarly, in the winter season, ML-based EMM results in 24% increased PES, 42% decreased PEC, and 24% increased GR for ED1 while 40% more PES, 53% less PEC, and 3% more GR for ED2 and 40% more PES, 53% less PEC, and 3% more GR for ED3. The efficiency of the ML algorithm (GPR) is cleared from the above-stated results. Critical analysis of SA-SLA designed in EMM concludes that smart SLAs with multiple ROC and ROD associates less PEC. Analysis of ML-based EMM and Optimization based EMM reveals that ML approach associates improved results of SA-SLA. Moreover, statistical tests and tabular analysis prove the effectiveness of our proposed ML approach in developing EMM for prosumers and smart grid. Finally, it is concluded that ML is an efficient tool to design an EMM model for bidirectional energy flow between ED prosumers and the smart grid. It is also concluded that optimization techniques are useful in calculating input covariates for the ML model to design ML-based EMM.

In future, we intend designing and analyzing ML-based energy management model incorporating prosumers clusters operating under SA-SLA. To prove the effectiveness of the outperforming ML algorithm, a comparative analysis of different ML algorithms will be presented. Moreover, to create competition among EDs, an incentive-based energy market will be developed and analyzed.

REFERENCES

- [1] D. Li and S. K. Jayaweera, "Machine-learning aided optimal customer decisions for an interactive smart grid," *IEEE Syst. J.*, vol. 9, no. 4, pp. 1529–1540, Dec. 2015.
- [2] M. Jawad, M. B. Qureshi, U. Khan, S. M. Ali, A. Mehmood, B. Khan, X. Wang, and S. U. Khan, "A robust optimization technique for energy cost minimization of cloud data centers," *IEEE Trans. Cloud Comput.*, early access, Nov. 7, 2018, doi: [10.1109/TCC.2018.2879948](https://doi.org/10.1109/TCC.2018.2879948).
- [3] A. M. Jadhav and N. R. Patne, "Priority-based energy scheduling in a smart distributed network with multiple microgrids," *IEEE Trans. Ind. Informat.*, vol. 13, no. 6, pp. 3134–3143, Dec. 2017.
- [4] S. Park, J. Lee, S. Bae, G. Hwang, and J. K. Choi, "Contribution-based energy-trading mechanism in microgrids for future smart grid: A game theoretic approach," *IEEE Trans. Ind. Electron.*, vol. 63, no. 7, pp. 4255–4265, Jul. 2016.
- [5] R. Kucęba, M. Zawada, M. Szajt, and J. Kowalik, "Prosumer energy as a stimulator of micro-smart grids development-on the consumer side," in *Proc. IOP Conf. Ser., Earth Environ. Sci.*, vol. 164, 2018, Art. no. 012003.
- [6] A. Hahn, R. Singh, C.-C. Liu, and S. Chen, "Smart contract-based campus demonstration of decentralized transactive energy auctions," in *Proc. IEEE Power Energy Soc. Innov. Smart Grid Technol. Conf. (ISGT)*, Apr. 2017, pp. 1–5.
- [7] Y. K. Renani, M. Ehsan, and M. Shahidehpour, "Optimal transactive market operations with distribution system operators," *IEEE Trans. Smart Grid*, vol. 9, no. 6, pp. 6692–6701, Nov. 2018.
- [8] I. Hussain, S. M. Ali, B. Khan, Z. Ullah, C. A. Mehmood, M. Jawad, U. Farid, and A. Haider, "Stochastic wind energy management model within smart grid framework: A joint bi-directional service level agreement (SLA) between smart grid and wind energy district prosumers," *Renew. Energy*, vol. 134, pp. 1017–1033, Apr. 2019.
- [9] C. Roldán-Blay, G. Escrivá-Escrivá, and C. Roldán-Porta, "Improving the benefits of demand response participation in facilities with distributed energy resources," *Energy*, vol. 169, pp. 710–718, Feb. 2019.
- [10] A. S. Farsangi, S. Hadayeghparast, M. Mehdinejad, and H. Shayanfar, "A novel stochastic energy management of a microgrid with various types of distributed energy resources in presence of demand response programs," *Energy*, vol. 160, pp. 257–274, Oct. 2018.
- [11] S. Choi and S.-W. Min, "Optimal scheduling and operation of the ESS for prosumer market environment in grid-connected industrial complex," in *Proc. IEEE Ind. Appl. Soc. Annu. Meeting*, Oct. 2017, pp. 1–7.
- [12] F. Pallonetto, M. De Rosa, F. Milano, and D. P. Finn, "Demand response algorithms for smart-grid ready residential buildings using machine learning models," *Appl. Energy*, vol. 239, pp. 1265–1282, Apr. 2019.
- [13] E. González-Romera, M. Ruiz-Cortés, M.-I. Milanés-Montero, F. Barrero-González, E. Romero-Cadaval, R. Lopes, and J. Martins, "Advantages of minimizing energy exchange instead of energy cost in prosumer microgrids," *Energies*, vol. 12, no. 4, p. 719, Feb. 2019.
- [14] A. Shahsavari, M. Farajollahi, E. M. Stewart, E. Cortez, and H. Mohsenian-Rad, "Situational awareness in distribution grid using micro-PMU data: A machine learning approach," *IEEE Trans. Smart Grid*, vol. 10, no. 6, pp. 6167–6177, Nov. 2019.
- [15] P. Gross, A. Salleb-Aouissi, H. Dutta, and A. Boulanger, "Ranking electrical feeders of the New York power grid," in *Proc. Int. Conf. Mach. Learn. Appl.*, Dec. 2009, pp. 359–365.
- [16] J.-S. Chou, S.-C. Hsu, N.-T. Ngo, C.-W. Lin, and C.-C. Tsui, "Hybrid machine learning system to forecast electricity consumption of smart grid-based air conditioners," *IEEE Syst. J.*, vol. 13, no. 3, pp. 3120–3128, Sep. 2019.
- [17] H. Lin, K. Sun, Z.-H. Tan, C. Liu, J. M. Guerrero, and J. C. Vasquez, "Adaptive protection combined with machine learning for microgrids," *IET Gener., Transmiss. Distrib.*, vol. 13, no. 6, pp. 770–779, Mar. 2019.
- [18] S. Ahmed, Y. Lee, S.-H. Hyun, and I. Koo, "Unsupervised machine learning-based detection of covert data integrity assault in smart grid networks utilizing isolation forest," *IEEE Trans. Inf. Forensics Security*, vol. 14, no. 10, pp. 2765–2777, Oct. 2019.
- [19] F. Riaz, S. Naem, R. Nawaz, and M. Coimbra, "Active contours based segmentation and lesion periphery analysis for characterization of skin lesions in dermoscopy images," *IEEE J. Biomed. Health Inform.*, vol. 23, no. 2, pp. 489–500, Mar. 2019.
- [20] S. Ayyaz, U. Qamar, and R. Nawaz, "HCF-CRS: A hybrid content based fuzzy conformal recommender system for providing recommendations with confidence," *PLoS ONE*, vol. 13, no. 10, Oct. 2018, Art. no. e0204849.
- [21] F. Anwaar, N. Iltaf, H. Afzal, and R. Nawaz, "HRS-CE: A hybrid framework to integrate content embeddings in recommender systems for cold start items," *J. Comput. Sci.*, vol. 29, pp. 9–18, Nov. 2018.
- [22] X. Wang, R. Rak, A. Restificar, C. Nobata, C. Rupp, R. T. B. Batista-Navarro, R. Nawaz, and S. Ananiadou, "Detecting experimental techniques and selecting relevant documents for protein-protein interactions from biomedical literature," *BMC Bioinf.*, vol. 12, no. 8, p. 11, Dec. 2011.

- [23] R. Nawaz, P. Thompson, and S. Ananiadou, "Negated bio-events: Analysis and identification," *BMC Bioinf.*, vol. 14, no. 1, p. 14, Dec. 2013.
- [24] M. S. Saleh, A. Althabani, Y. Esa, Y. Mhandi, and A. A. Mohamed, "Impact of clustering microgrids on their stability and resilience during blackouts," in *Proc. Int. Conf. Smart Grid Clean Energy Technol. (ICSGCE)*, Oct. 2015, pp. 195–200.
- [25] H. Qadir, O. Khalid, M. U. S. Khan, A. U. R. Khan, and R. Nawaz, "An optimal ride sharing recommendation framework for carpooling services," *IEEE Access*, vol. 6, pp. 62296–62313, 2018.
- [26] R. Nawaz, P. Thompson, J. McNaught, and S. Ananiadou, "Meta-Knowledge Annotation of Bio-Events," in *Proc. LREC*, vol. 17, 2010, pp. 2498–2507.
- [27] (Nov. 19, 2019). *National Institute of Standards and Technology*. Accessed: Nov. 25, 2019. [Online]. Available: <https://www.nist.gov/>
- [28] E. Kabalci and Y. Kabalci, *Smart Grids and Their Communication Systems*. Singapore: Springer, 2019.
- [29] Z. Chen, M. Sim, and P. Xiong, "Robust stochastic optimization made easy with R SOME," *Manage. Sci.*, vol. 66, no. 8, pp. 3329–3339, 2020.
- [30] B. Manobel, F. Sehnke, J. A. Lazzús, I. Salfate, M. Felder, and S. Montecinos, "Wind turbine power curve modeling based on Gaussian processes and artificial neural networks," *Renew. Energy*, vol. 125, pp. 1015–1020, Sep. 2018.
- [31] G. Wang, Z. Tan, Q. Tan, S. Yang, H. Lin, X. Ji, D. Gejirifu, and X. Song, "Multi-objective robust scheduling optimization model of wind, photovoltaic power, and BESS based on the Pareto principle," *Sustainability*, vol. 11, no. 2, p. 305, Jan. 2019.
- [32] F. Magrassi, E. Rocco, S. Barberis, M. Gallo, and A. D. Borghi, "Hybrid solar power system versus photovoltaic plant: A comparative analysis through a life cycle approach," *Renew. Energy*, vol. 130, pp. 290–304, Jan. 2019.
- [33] J. Cao, Z. Bu, Y. Wang, H. Yang, J. Jiang, and H.-J. Li, "Detecting prosumer-community groups in smart grids from the multiagent perspective," *IEEE Trans. Syst., Man, Cybern. Syst.*, vol. 49, no. 8, pp. 1652–1664, Aug. 2019.
- [34] W. Tushar, T. K. Saha, C. Yuen, T. Morstyn, M. D. McCulloch, H. V. Poor, and K. L. Wood, "A motivational game-theoretic approach for peer-to-peer energy trading in the smart grid," *Appl. Energy*, vol. 243, pp. 10–20, Jun. 2019.
- [35] L. Ma, N. Liu, J. Zhang, and L. Wang, "Real-time rolling horizon energy management for the Energy-Hub-Coordinated prosumer community from a cooperative perspective," *IEEE Trans. Power Syst.*, vol. 34, no. 2, pp. 1227–1242, Mar. 2019.
- [36] S. Mirjalili, *Evolutionary Algorithms and Neural Networks* (Studies in Computational Intelligence). Cham, Switzerland: Springer, 2019.
- [37] F. Lane, R. M. A. Azad, and C. Ryan, "DICE: Exploiting all bivariate dependencies in binary and multary search spaces," *Memetic Comput.*, vol. 10, no. 3, pp. 245–255, Sep. 2018.
- [38] R. M. A. Azad and C. Ryan, "A simple approach to lifetime learning in genetic programming-based symbolic regression," *Evol. Comput.*, vol. 22, no. 2, pp. 287–317, Jun. 2014.
- [39] R. Yunus, O. Arif, H. Afzal, M. F. Amjad, H. Abbas, H. N. Bokhari, S. T. Haider, N. Zafar, and R. Nawaz, "A framework to estimate the nutritional value of food in real time using deep learning techniques," *IEEE Access*, vol. 7, pp. 2643–2652, 2019.
- [40] H. Waheed, S.-U. Hassan, N. R. Aljohani, J. Hardman, S. Alelyani, and R. Nawaz, "Predicting academic performance of students from VLE big data using deep learning models," *Comput. Hum. Behav.*, vol. 104, Mar. 2020, Art. no. 106189.
- [41] G. Chennupati, R. M. A. Azad, and C. Ryan, "Multi-core GE: Automatic evolution of CPU based multi-core parallel programs," in *Proc. Conf. Companion Genetic Evol. Comput. Companion*, 2014, pp. 1041–1044.
- [42] G. Chennupati, R. M. A. Azad, and C. Ryan, "Performance optimization of multi-core grammatical evolution generated parallel recursive programs," in *Proc. Genetic Evol. Comput. Conf. (GECCO)*, 2015, pp. 1007–1014.
- [43] Climate Interpreter. *U.S. Energy Information Administration Energy Profile by State | Climate Interpreter*. Accessed: Feb. 9, 2020. [Online]. Available: <https://climateinterpreter.org/resource/us-energy-information-administration-energy-profile-state>



WAQAR AHMED (Associate Member, IEEE) received the B.S. degree in electrical power engineering from Bahauddin Zakariya University, Multan, Pakistan, in 2017. He is currently pursuing the M.S. degree in electrical engineering with the COMSATS University Islamabad, Abbottabad Campus, Abbottabad, Pakistan.

His research interests include service level agreement based energy management model for smart grids and optimization technique for power distribution.



HAMMAD ANSARI received the B.S. degree in electronics and electrical engineering from the University of Glasgow, U.K.

He is an ERC with research interests in nano-electronics, data analysis and statistics, as well as clean/renewable energy sources.



BILAL KHAN received the M.S. and Ph.D. degrees in control systems from The University of Sheffield, U.K., in 2007 and 2013, respectively.

He is currently working as an Assistant Professor with the Electrical and Computer Engineering Department, COMSATS University Islamabad, Abbottabad Campus, Abbottabad, Pakistan. His research interests include control systems and optimization.



ZAHID ULLAH received the B.S. and M.S. degrees in electrical engineering from UET Peshawar and COMSATS University Islamabad, Abbottabad Campus, Abbottabad, Pakistan, respectively.

He is currently working as a Lecturer with UMT Lahore, Pakistan. His research interests include smart grid, high voltage systems, and power system stability.



SAHIBZADA MUHAMMAD ALI received the B.S. and M.S. degrees in electrical engineering from the University of Engineering and Technology, Peshawar, Pakistan, in 2007 and 2010, respectively, and the Ph.D. degree from North Dakota State University, Fargo, ND, USA, in 2015.

He is currently working as an Assistant Professor with the Electrical and Computer Engineering Department, COMSATS University Islamabad, Abbottabad Campus, Abbottabad, Pakistan.

His research interests include smart grid, power systems, grid-interfaced wind models, control systems, electrical drives, and biomedical.



CHAUDHRY ARSHAD ARSHAD MEHMOOD received the B.S. degree from CECOS University Peshawar, Pakistan, in 2001, the M.S. degree in control systems from The University of Sheffield, U.K., in 2007, and the Ph.D. degree from North Dakota State University, Fargo, ND, USA, in 2014.

He is currently working as an Assistant Professor with the Electrical and Computer Engineering Department, COMSATS University Islamabad, Abbottabad Campus, Abbottabad, Pakistan. His research interests include electrical machine drives and control systems.



MUHAMMAD B. QURESHI (Member, IEEE) received the B.S. and M.S. degrees in computer engineering from COMSATS University Islamabad, Abbottabad Campus, Abbottabad, Pakistan, in 2007 and 2010, respectively, and the Ph.D. degree from North Dakota State University, Fargo, ND, USA, in 2017.

He is currently working as an Assistant Professor with the Electrical and Computer Engineering Department, COMSATS University Islamabad, Abbottabad Campus, Abbottabad, Pakistan. His research interests include control systems, optimization, and biomedical engineering.



IQRAR HUSSAIN received the B.S. and M.S. degrees in electrical engineering from UET Peshawar and COMSATS IIT Abbottabad, Pakistan, respectively.

His research interests include smart grid, optimization techniques, and renewable energy systems. He is currently a Lecturer with UMT Lahore, Pakistan.



MUHAMMAD JAWAD received the B.Sc. degree in computer engineering from COMSATS University Islamabad, Lahore Campus, in 2007, the M.Sc. degree from The University of Manchester, U.K., in 2009, and the Ph.D. degree from North Dakota State University, Fargo, ND, USA, in 2015. He is currently working as an Assistant Professor with COMSATS University Islamabad, Lahore Campus, Lahore, Pakistan.

His research interests include optimization theory, prediction algorithms, machine learning, cloud computing, and smart grids optimization for energy efficiency.



MUHAMMAD USMAN SHAHID KHAN (Member, IEEE) received the Ph.D. degree from North Dakota State University, Fargo, ND, USA.

He is currently an Assistant Professor with COMSATS University Islamabad, Abbottabad Campus, Abbottabad, Pakistan. His areas of interests are cloud computing, smart grids, data mining, big data, and network security.



AMJAD ULLAH received the master's degree in computer security from George Washington University, USA, and the Ph.D. degree in electrical power engineering from Peshawar, in 2010.

He joined the University of Engineering and Technology in 1993. He is currently working as a Professor with the Electrical Engineering Department. He remained as a member of the Board of Directors in PESCO, where he was actively involved in managing energy related polices for the company.



RAHEEL NAWAZ is currently the Director of Digital Technology Solutions and a Reader in Analytics and Digital Education with the Manchester Metropolitan University (MMU).

He has founded and/or headed several research units specializing in artificial intelligence, data science, digital transformations, digital education, and apprenticeships in higher education. He has led on numerous funded research projects in the U.K., EU, South Asia, and Middle East. He has held adjunct or honorary positions with several research, higher education, and policy organizations, both in the U.K. and overseas. He regularly makes media appearances and speaks on a range of topics, especially in artificial intelligence and higher education.

...